SYNTHESIS OF DICATIONIC IONIC LIQUIDS AND THEIR APPLICATION AS CO-CATALYST FOR FRUCTOSE CONVERSION

SUHAILA BINTI MOHD YAMAN

FACULTY OF SCIENCE
UNIVERSITY OF MALAYA
KUALA LUMPUR

2018

SYNTHESIS OF DICATIONIC IONIC LIQUIDS AND THEIR APPLICATION AS CO-CATALYST FOR FRUCTOSE CONVERSION

SUHAILA BINTI MOHD YAMAN

DISSERTATION SUBMITTED IN FULFILMENT OF THE REQUIREMENTS FOR THE DEGREE OF MASTER OF SCIENCE

DEPARTMENT OF CHEMISTRY
FACULTY OF SCIENCE
UNIVERSITY OF MALAYA
KUALA LUMPUR

2018

UNIVERSITY OF MALAYA
ORIGINAL LITERARY WORK DECLARATION

Name of Candidate: Suhaila Binti Mohd Yaman

Matric No: SGR140027

Name of Degree: Master of Science

Title of Project Paper/Research Report/Dissertation/Thesis ("this Work"):

Synthesis of Dicationic Ionic Liquids and Their Application as Co-Catalyst for

Fructose conversion.

Field of Study: Inorganic Chemistry

I do solemnly and sincerely declare that:

(1) I am the sole author/writer of this Work;
(2) This Work is original;
(3) Any use of any work in which copyright exists was done by way of fair dealing and for permitted purposes and any excerpt or extract from, or reference to or reproduction of any copyright work has been disclosed expressly and sufficiently and the title of the Work and its authorship have been acknowledged in this Work;
(4) I do not have any actual knowledge nor do I ought reasonably to know that the making of this work constitutes an infringement of any copyright work;
(5) I hereby assign all and every right in the copyright to this Work to the University ofMalaya ("UM"), who henceforth shall be owner of the copyright in this Work and that any reproduction or use in any form or by any means whatsoever is prohibited without the written consent of UM having been first had and obtained;
(6) I am fully aware that if in the course of making this Work I have infringed any copyright whether intentionally or otherwise, I may be subject to legal action or any other action as may be determined by UM.

Candidate's Signature   Date:

Subscribed and solemnly declared before,

Witness's Signature   Date:

Name:

Designation:

SYNTHESIS OF DICATIONIC IONIC LIQUIDS AND THEIR APPLICATION AS CO-CATALYST FOR FRUCTOSE CONVERSION

ABSTRACT

In this study, six new imidazolium based dicationic ionic liquids (ILs) were successfully synthesized with one step process. These ILs were designated with three different positions of substituent of benzyl-imidazolium at ortho, meta and para on cationic site while tuning the counter anion with chloride and hydrogen sulphate anion. As a result, this unique combination between cation and anion dramatically impact towards the properties of ILs. The characterizations of all ILs were elucidated using ^{1}H-NMR, ^{13}C-NMR, FT-IR and CHN elemental analyses. The thermal analysis of these ILs reveals the information of phase transition of glass transition (T_g), melting temperature (T_m), decomposition temperature (T_d) and their high thermal stability. Further, the acidity properties were quantified by Hammet acidity function (H_o) that gives the information on the acidity strength of each ILs. These ILs also meet the criteria as catalyst as they were hydrophilic, high stability, acidic and can be recycled. The investigation was started with the screening process by using each IL as a catalyst in separate reaction. Each parameter such as time, temperature, catalyst loading was optimized and the transformation mechanism of fructose to HMF was rationalized. Besides, the reusability study had also been conducted. In addition, in–situ study by using ^{1}H-NMR provides information on the selectivity of the ILs at a given time and temperature. The intrinsic properties of dipole moment and polarity that existed in the structural ILs were also discussed. The difference in position of ortho, meta and para substituent was proven to give a significant contribution and affecting the fructose dehydration process.

Keywords: Dicationic ionic liquids, ortho-meta-para position, fructose

SINTESIS DWIKATIONIK CECAIR IONIK DAN PENGGUNAANYA SEBAGAI PEMANGKIN BERSAMA UNTUK PENUKARAN FRUKTOSA

ABSTRAK

Dalam kajian ini, enam cecair dwikationik (ILs) imidazolium baru telah berjaya disintesis dengan satu proses tindak balas. ILs telah direka dengan tiga kedudukan kumpulan gantian benzil-imidazol yang berbeza iaitu pada kedudukan ortho, meta dan para dwikationik sementara klorida dan hydrogen sulfide asebagai pasangan anionik. Keputusan menunjukkan kombinasi unik antara kationik dan anionic memberi impak dramatic pada sifat-sifat mereka. Pencirian semua ILs telah dijelaskan menggunakan ^{1}H-NMR, ^{13}C-NMR, FT-IR dan CHN analisis unsur. Analisis termal ILs ini mendedahkan maklumat berkaitan suhu peralihan kaca (T_g), suhu lebur (T_m), suhu penguraian (T_d) dan kestabilan haba yang tinggi. Selanjutnya, sifat-sifat keasidan telah dinilai oleh fungsi keasidan Hammet (H_o) yang memberi maklumat mengenai kekuatan keasidan setiap ILs. Selain itu, ILs ini juga memenuhi criteria sebagai pemangkin kerana mempunyai sifat bahan hidrofilik, kestabilan tinggi, berasid dan boleh digunakan semula. Proses kajian telah dimulakan dengan proses saringan dengan menggunakan setiap ILs sebagai pemangkin di dalam tindakbalas berasingan. Setiap parameter seperti masa, suhu, dos pemangkin dioptimumkan dan transformasi fruktosa ke HMF dirasionalkan. Selain itu, kajian kebolehgunaan semula ILs juga telah dijalankan. Tambahan pula, kajian in-situ dengan menggunakan ^{1}H-NMR memberikan gambaran yang jelas mengenai pemilihan ILs dalam satu masa dan suhu tertentu. Sifat-sifat intrinsik momen dwikutub dan kekutuban yang wujud dalam struktur ILs juga dibincangkan dan perbezaan pada kedudukan gantian ortho, meta dan para telah terbukti memberikan sumbangan yang penting dan memberi kesan kepada proses dehidrasi fruktosa.

Katakunci: dwikationik cecair ionik, kedudukan ortho-meta-para, fruktosa.

ACKNOWLEDGEMENTS

TABLE OF CONTENTS

LIST OF FIGURES

LIST OF SCHEMES

LIST OF TABLES

LIST OF SYMBOLS AND ABBREVIATIONS

A-orthoCl	:	3,3'-(1,4-phenylenebis(methylene))bis(1-benzyl-1H-imidazol-3-ium) hydrogen sulfate
A-orthoHSO$_4$	:	3,3'-(1,2-phenylenebis(methylene))bis(1-benzyl-1H-imidazol-3-ium) hydrogen sulfate
[Bmim][BF$_4$]	:	1-butyl-3-methylimidazolium tetrafluoroborate
[Bmim][Cl]	:	1-butyl-3-methylimidazolium chloride
B-paraCl	:	3,3'-(1,4-phenylenebis(methylene))bis(1-benzyl-1H-imidazol-3-ium) dichloride
B-paraHSO$_4$	:	3,3'-(1,4-phenylenebis(methylene))bis(1-benzyl-1H-imidazol-3-ium) hydrogen sulfate
C-metaCl	:	3,3'-(1,2-phenylenebis(methylene))bis(1-benzyl-1H-imidazol-3-ium) dichloride
C-metaHSO$_4$	:	3,3'-(1,3-phenylenebis(methylene))bis(1-benzyl-1H-imidazol-3-ium) hydrogen sulfate
CO	:	Carbon monoxide
DAD	:	Diode Array Detector
DF	:	Dilution factor
DMA	:	Dimethylacetylamide
DMFA	:	Dimethylformamide
DMSO	:	Dimethylsulfoxide
ELSD	:	Evaporative Light Scattering Detector
[Emim][Cl]	:	1-ethyl-3-methylimidazolium chloride
EWG	:	Electron withdrawing group
FA	:	Formic acid
HMF	:	5-hydroxymethylfurfural
H$_o$	:	Hammett value
HPLC	:	High Performance Liquid Chromatography

ILs	:	Ionic liquids
LA	:	Levulinic acid
NO_x	:	Nitrogen oxides
SO_x	:	Sulphur oxides
T_d	:	Decomposition temperature
T_g	:	Glass transition temperature
T_m	:	Melting temperature
UV	:	Ultraviolet visible spectroscopy
μ	:	Dipole moment

CHAPTER 1: INTRODUCTION

1.1 Background of study

Alternative and renewable energy sources such as wind, solar, geothermal, and biomass have become increasingly attractive for use to reduce or replace fossil fuel consumption and to produce more competitive resources. In fact, the concepts of sustainable development, renewable resources, green energy and eco-friendly processes are some of the main focuses in developing and industrializing country (Demirbas, 2008).

Biomass is an attractive and promising feedstock for three important reasons (Demirbas, 2008). First, it is a renewable resource that could be sustainably developed in the future. Second, energy generation from biomass is a carbon neutral process and it only releases a very small amount of sulphur. Finally, it gives significant economic potential that associated with diversifying energy sources resulting in technology impact as it being increasingly adopted and perhaps replace the consumption of fossil fuels in the future (Cadenas & Cabezudo, 1998). Briefly, biomass can be derived from crops and forest residues, animal waste, wood and herbaceous plants. Biomass can be converted into liquid and gaseous fuel through the thermochemical or biological route (Vasudevan et al., 2005).

Recently, biomass-derived 5-hydroxymethylfurfural (HMF) has garnered attention to meet the needs of chemicals with important application as alternative fuels (James et al., 2010). The yield of HMF from sugar can be optimized with respect to catalyst, solvent, substrate, reaction time, and temperature.

ILs are invaluable in the development of environmentally friendly technologies for producing chemicals and fuel from non-fossil carbon sources (Saha & Abu-Omar, 2014). ILs offer some unique properties such as excellent thermal stability, negligible volatility and flammability, (Seddon et al., 2000) and reusability (Ma et al., 2015; Qi et al., 2011; Varma & Namboodiri, 2001). ILs have been used in applications such as carbon capture

(Raja Shahrom et al., 2016; Zhang et al., 2012), nuclear fuel reprocessing (Ha et al., 2010), biomass processing (Tan & MacFarlane, 2010), catalytic reactions (Ratti, 2014), pharmaceuticals (Marrucho et al., 2014), waste recycling (Chiappe & Pieraccini, 2005; Huddleston & Rogers, 1998; Nakashima et al., 2005), and batteries (De Souza et al., 2003; Lu et al., 2002; Yuan et al., 2006; Zakeeruddin & Graetzel, 2009). Their versatility is due to the large number of possible combinations of cations and anions that can be tailored to their specific application.

To date, various modifications have been made to ILs according to the needs and desire application. Dicationic ILs have been reported to be more effective and versatile than conventional monocationic ILs (Chinnappan & Kim, 2012). The effectiveness of dicationic ILs is highlighted in the works of Ishida & Shirota (2013) and Shirota et al. (2011). Both studies have benefit from higher intra- and intermolecular interaction associated with dicationic ILs. Chinnappan et al. (2014) reported that dicationic ILs showed excellent catalytic activity due to extensive hydrogen bonding which promotes dissolution of the substrate during reaction. Therefore, dicationic ILs are an efficacious medium for use in reactions and they are utilized in this study as catalyst.

Our research focuses on the design and synthesis of dicationic ILs which differ in their position and their catalytic ability for the dehydration of fructose to 5-hydroxymethylfurfural (HMF). Five points must be considered when using the dicationic ILs as catalyst in dehydration reaction i) its physicochemical properties, ii) cation and anion species, iii) mechanism and interaction with fructose (Ståhlberg et al., 2011), iv) symmetry (Kotadia & Soni, 2013), and v) chain length (Jadhav et al., 2012). This study aims to correlate the geometry of the ILs (ortho, meta and para) to its catalytic performance for the development of an effective process for fructose dehydration.

1.2 Research objectives

The objectives of this study are:

- To synthesize and characterize new dicationic ionic liquids based imidazolium.

- To employ these new ILs as catalyst in dehydration of fructose to 5-hydroxymethylfurfural.

- To quantify the percentage of conversion, percentage of yield and selectivity of fructose and 5-hydroxymethylfurfural.

- To propose the reaction mechanism reaction between catalyst and fructose.

2.1 What is HMF?

Cellulose and hemicelluloses are the most abundant organic content in biomass material. Therefore, it becomes attractive to utilize them as a source of energy or as precursor materials in chemical synthesis (Anwar et al., 2014; Bajpai, 2016). The biggest challenge to overcome is to produce 5-hydroxymethylfurfural (HMF) from biomass through simple chemical routes (Saha & Abu-Omar, 2014). **Scheme 2.1** presents the broad range of valuable chemicals that can simply be derived from biomass using HMF as the precursor.
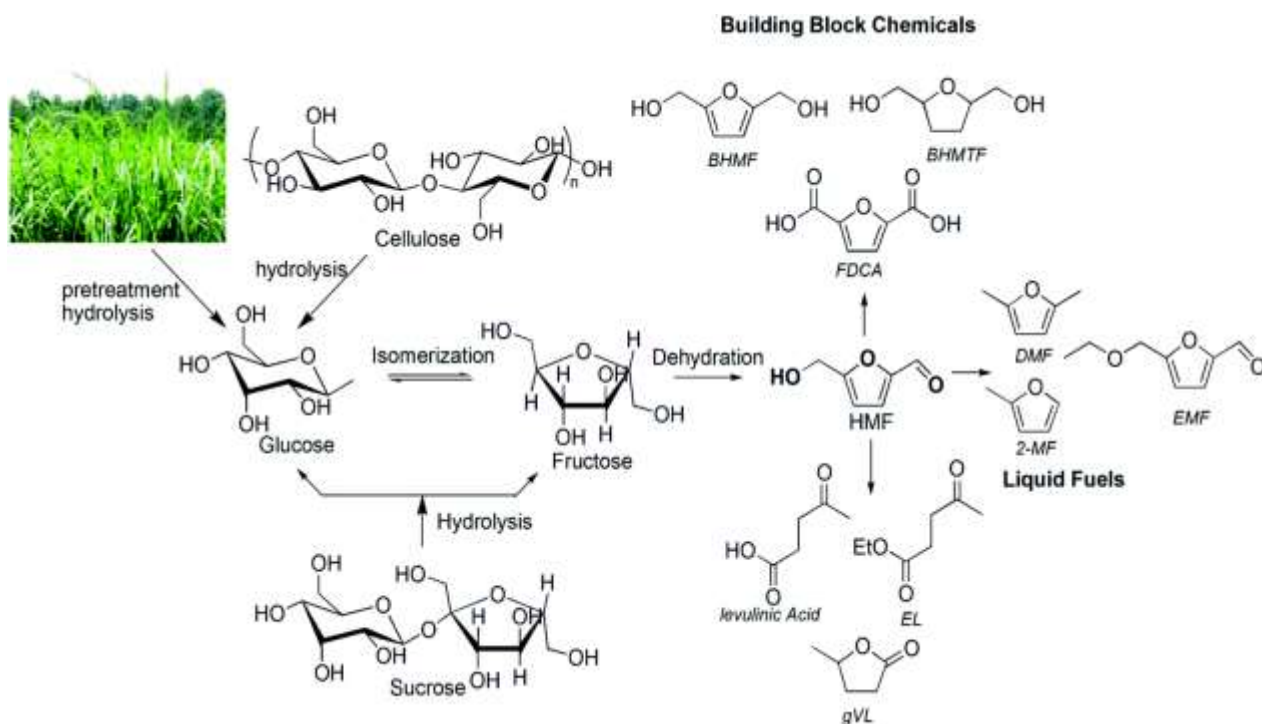
Scheme 2.1: Valuable chemicals produced from biomass (Saha & Abu-Omar, 2014).

HMF is an organic compound belonging to the class of furans. The molecule is a furan ring system with an aldehyde and a hydroxymethyl group at the 2 and 5 positions respectively. HMF is also classified as one of the best building block chemicals that are derived from biomass according to the U.S Department of Energy (Zakrzewska et al., 2011). It is an important compound in bridging carbohydrate chemistry and mineral oil based industrial organic chemistry. Typically, the synthesis of HMF is based on a

dehydration process that involves high temperatures and acidic conditions (Zakrzewska et al., 2011).

2.1.1 Dehydration of fructose

Dehydration of fructose is a process where three mols of water are removed from one mol of fructose to form one mol of HMF. This process can be conducted in various solvents such as water (De et al., 2011), dimethylsulfoxide (DMSO) (Tong & Li, 2010), dimethylformamide (DMFA) (Ohara et al., 2010), dimethylacetylamide (DMA), poly (glycol ether) (Kishi et al., 2011) and supercritical solvents or their mixture (water, acetone, methanol, or acetic acid) (Cantero et al., 2015; Kruse & Dahmen, 2015; Savage et al., 1995). The selection of the solvent is important as it influences the fructose conversion, HMF yield, and separation process. Furthermore, the correct choice of solvent can help suppress undesirable side products such as levulinic acid, formic acid and humins (Van Zandvoort et al., 2013). These possible side products are highlighted in **Scheme 2.2**.

Generally, the reaction efficiency depends on the type of catalysts used while the reaction activity is controlled by the temperature, reaction time, and solvent used. The catalysts that have been used in the reaction include salts, mineral and organic acids (Tuteja et al., 2014), zeolites (Nikolla et al., 2011), ion exchange resins (Qi et al., 2008) and ionic liquids (Zhang & Zhao, 2010). In general, the catalyst used today only produces a low yield of product, and the kinetic progression of the fructose conversion is debatable. Previous researchers (Jae et al., 2010; Pagán et al., 2012) have suggested two important pathways for the dehydration reaction; the isomerization using HCl or direct conversion using metal chloride as a catalyst. A fundamental understanding of catalyst, is a key step in understanding the catalytic activity that impact HMF production.
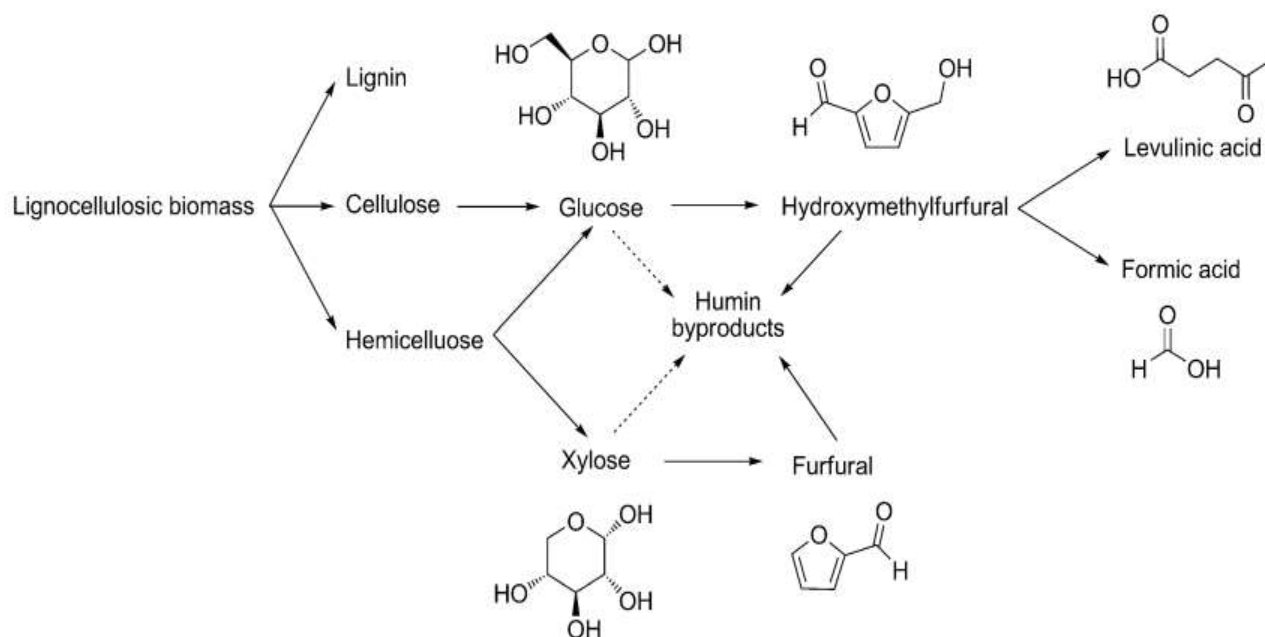
Scheme 2.2: Production of chemicals from lignocellulosic biomass and the related formation of side products (Van Zandvoort et al., 2013).

2.2 Ionic liquids

Ionic liquids (ILs) are organic salts that composed by combination of a large organic cation (i.e. imidazolium, pyrrodium, pyridinium, phosphonium) and an inorganic anion (i.e. halide, nitrite, acetate, hydrogen sulphate). Due to large possible combination of cations and anions, ILs have been successfully used in different application such as solvent and catalyst in specific chemical reactions. **Figure 2.1** and **2.2** illustrate the common cations and anions used in ILs. **Table 2.1** lists the advantages of ILs (Kunz & Häckl, 2016).
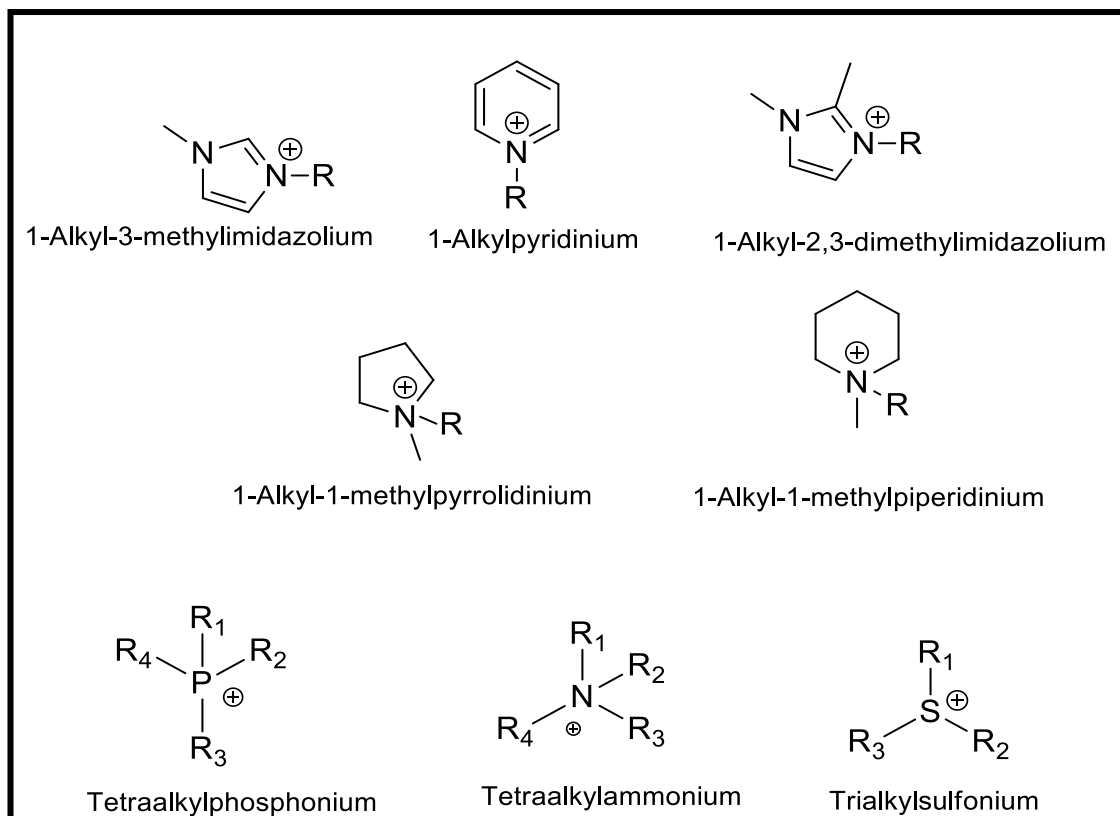
Figure 2.1: Examples of most commonly described ILs cations (Zakrzewska et al., 2011).
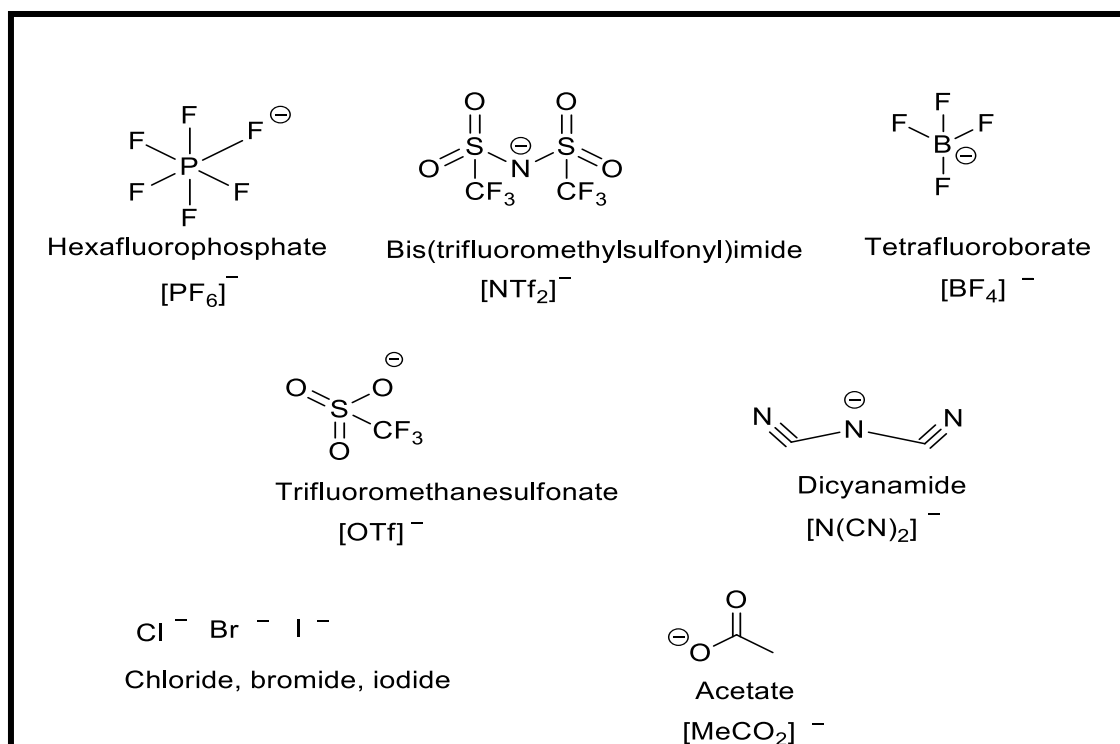
Figure 2.2: Examples of most commonly described ILs anions (Zakrzewska et al., 2011).

Table 2.1: The advantages of ILs.

No	Advantages	Remarks
1	Number of imaginable combination cation and anion	High number of up to 10^{18} possible combinations.
2	Tunability	Designer solvents tunable by varying functional groups or alkyl chain length
3	Vapour pressure	Negligible vapour pressure at normal conditions; almost no emission to the atmosphere
4	Flammability	Usually non-flammable
5	Stability	Thermostable in a wide temperature range; stable against electrochemical decomposition in wide potential range.

2.2.1 ILs as designer solvent

One of the fascinating advantages of ILs is they have enormous combination of cationic and anionic. Therefore, this tunable property makes them as designer solvent that relevant in various types of application (Shukla et al., 2011). Moreover, the unique properties of ILs arises from the fact that the anion and cation species not only form ionic and covalent bonds, but also relatively weaker interactions such as hydrogen bonding, Columbic interaction and π stacking (Anderson et al., 2002; Holbrey et al., 2003; Shukla et al., 2011). The effects of the cation and anion on ILs properties are summarized in **Table 2.2** (Duarte, 2009).

Table 2.2: Effects of anion and cation constituents in ILs properties.

No	Properties	Effect of cation	Effect of anion
1	Water solubility	Hydrophobicity increase with increase of alkyl chain length	Strongly depend on anion type such as $[PF_6]^-$ and $[NTf_2]^-$ hydrophobic. $[Cl]^-$ and $[Br]^-$ are hydrophilic.
2	Polarity	Strongly depend on cation type	Anion type has less influence
3	Viscosity	Increase with increasing of the cation size	No definite pattern
4	Density	Decrease with increasing of the cation	No definite pattern
5	Conductivity	Conductivity decrease with increase of alkyl chain	-

2.2.2 ILs as catalyst for dehydration reaction

In one early report regarding HMF production from fructose, commercialized ILs which is 1-butyl-3-methylimidazolium chloride [BMIM][Cl] was employed as solvent with a sulfonic ion exchange resin as the catalyst. The result showed 98.6 % fructose conversion and 83.2 % HMF yield (Qi et al., 2009). The reaction was conducted for 10 min at 80 °C. Further, comparison study with 1-butyl-3-methylimidazolium tetrafluroborate [BMIM][BF$_4$] but it resulted in lower efficiency and selectivity. This observation can be rationalized by the greater hydrogen bonding strength and nucleophilic character of chloride ion. Another study compared the choice of cation between the systems of [BMIM][Cl]/sulfonic acid and 1-ethyl-3-methylimidazolium chloride [EMIM][Cl]/sulfonic acid. The data analysis revealed that the [EMIM][Cl] which had a less bulky cation resulted in a higher production of HMF. This could be due to the better accessibility of the electrophile during the dehydration reaction (Imteyaz Alam et al., 2012).

Despite of using ILs as solvent, previous works also reported that ILs is also extensively used as a catalyst with the aid of various solvents (Imteyaz Alam et al., 2012;

Jadhav et al., 2013). The role of the solvent is to provide a homogeneous medium for reaction. A vast majority of studies make use of acidic ILs (De et al., 2011; Imteyaz Alam et al., 2012; Li et al., 2010). In this context, the abundance of protons (H^+) can remove the –OH group efficiently from the fructose to form HMF. Common acidic anion species include hydrogen sulfate (HSO_4^-), triflate ($CF_3SO_3^-$), tetrafluoroborate (BF_4^-), metal chloride and chloride (Cl^-). **Scheme 2.3** illustrates the dehydration process under acidic conditions.
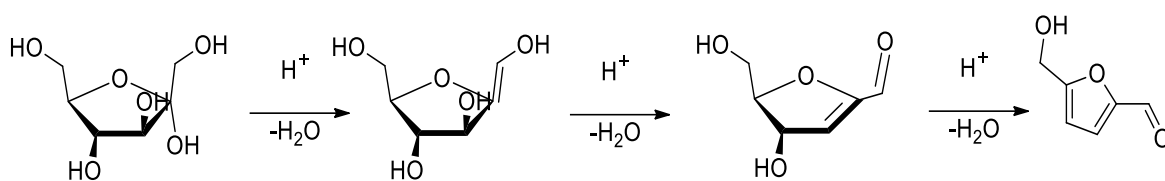
Scheme 2.3: The transformation fructose to HMF in acidic condition (Imholf & Van der Waal, 2013).

To date, several studies have begun to examine thoroughly the microscopic structure of the ILs that involved in dehydration reaction. Detailed analysis by Ståhlberg et al. (2011), has emphasized few points that need more attention including, the influence of the cation and anion of the ILs on the reaction, the study of physicochemical properties of ILs and the mechanism pathway of the interactions between ILs and starting materials. The ILs (**Figure 2.3)** appears to affect their physicochemical properties such as melting point, decomposition temperature and acidity. In general, asymmetric ILs structures exhibit very high stability, acidity, and catalytic activity for the dehydration of fructose. The excellent performance of the asymmetric ILs can be explained by its unique structure that enables the activation of the C-OH bond in fructose. Furthermore, the design of the structure allows for better accessibility of the cation which is an important step to initiate the reaction mechanism (Kotadia & Soni, 2013).
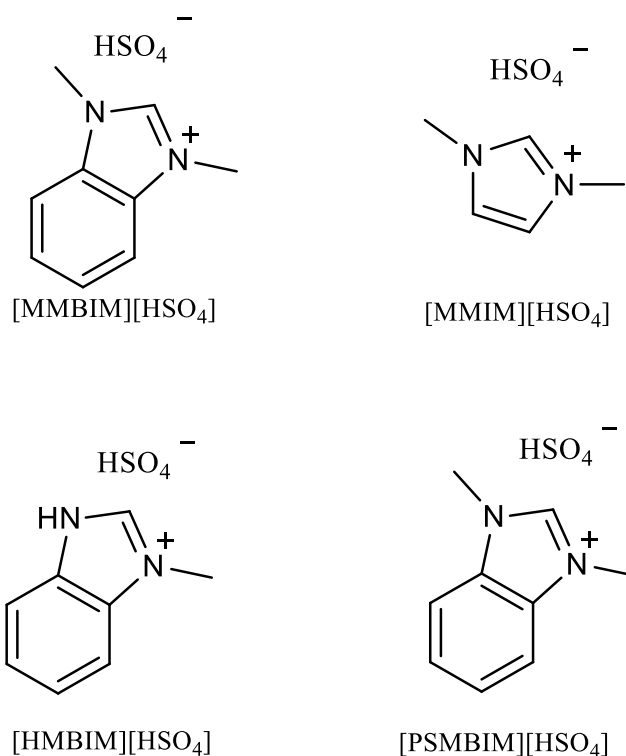
Figure 2.3: Symmetry and asymmetry monocationic ILs used in dehydration of fructose (Jadhav et al., 2012).

There has been a vast investigation regarding the impact of chain length of the ILs in the dehydration reaction system. Recent study by Jadhav et al. (2012) demonstrated their new hydrophilic dicationic ILs as catalysts and solvents for fructose dehydration. In their study, they manipulated the linkers between two imidazolium rings using di-, tri-, or tetra-ethylene glycol chains **(Scheme 2.4)**. The results revealed that the longer the ethylene glycol chains, the more effective of a catalyst in the production of HMF. It is due to the increase in hydrogen bonding linkage which promoted the high dissolution of sugar. In fact, the acidic anion was revealed to be important in forming a high degree of hydrogen bonds with the substrate.
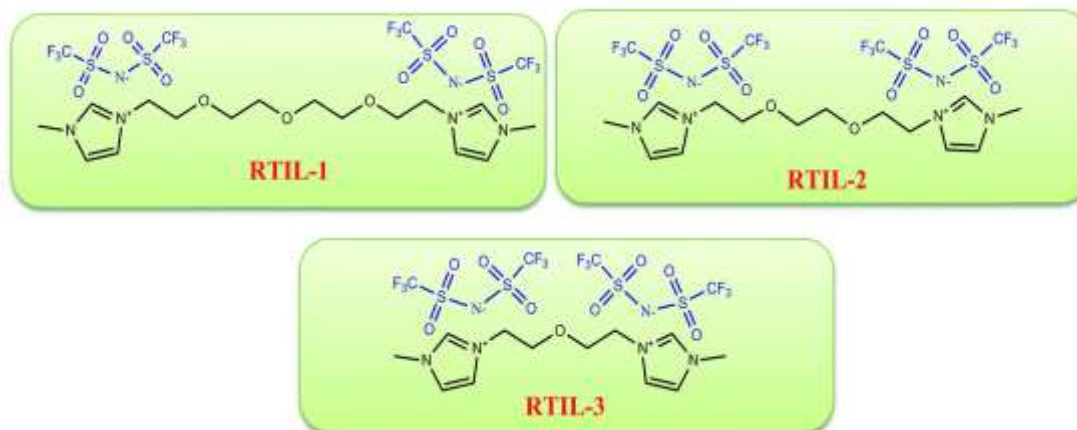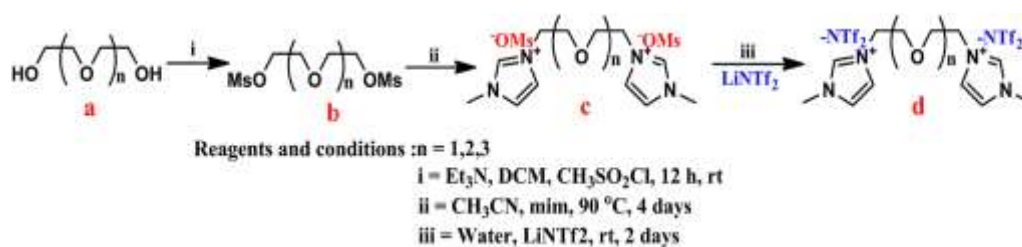
Scheme 2.4: Dicationic ILs with different alkyl chain length for dehydration of fructose. (Jadhav et al., 2012).

Collectively, these studies outline the critical role of ILs structure in many aspects. These findings bring significant contribution to the development and tailoring of an effective catalyst for dehydration process, although there is an extensive works on the structure effect of ILs on HMF yield. To the best of our knowledge there has not been a study that addressed the geometry effect of ILs on the dissolution of sugar and consequently, HMF production.

2.3 DMSO as important medium in dehydration reaction

DMSO is a polar molecule where the sulphur part of the molecule is electrophilic and the oxygen part is nucleophilic. A significant analysis and discussion regarding this subject was presented by Musau and Munavu in 1987. In the dehydration of fructose, levulinic and formic acid are the major by-products that affect the production of HMF. At optimized conditions, DMSO can suppress these by-products by associating with fructose and water as soon as they are produced. Consequently, the reaction is more

selective for HMF production when DMSO is used instead of other solvents such as water, acetonitrile, and methanol (Musau & Munavu, 1987).

Interestingly, this solvent also has been reported to produce HMF without the need of a catalyst (Amarasekara et al., 2008). The electrophilicity and nucleophilicity of DMSO play an important role in the isomerization of glucose into fructose through synergistic activation. The observation from this study is eventually possesses a question regarding the catalytic sites that necessary for this reaction to occur. The clues for this question lies on the mechanism study that shown by NMR which had revealed that the anomericity of D-fructose changes when it is heated from room temperature to 150 °C in DMSO. Critical analysis revealed the existence of an intermediate structure, (4R,5R)-4-hydroxy-5-hydroxymethyl-4,5-dihydrofuran-2-carbaldehyde before the formation of the end product HMF.

Referring to **Scheme 2.5**, the dehydration of fructose to HMF is initiated through simultaneous activation of OH group on the C2 of fructose (**Figure 2.4**) by the electrophilic end of DMSO and hydrogen bonding between the C1 of fructose and the nucleophilic end of DMSO resulting in the elimination of the first water molecule. The proton and oxygen exchange with DMSO is a facile process. Then, another two water molecules is removed by the nucleophilic oxygen at the centre of the DMSO molecule. As a result, this current finding adds to a growing body of literature especially on designing high performance catalysts for HMF production.

However, a major drawback in using DMSO as both the solvent and catalyst is that the transformation of fructose to HMF was only achieved at a high temperature of 150 °C. This is a concern because it is close to the boiling point of DMSO which is 160 °C. This leads to instability in the reaction media, decomposition, and inefficiency in product separation (Imhof & van der Waal, 2013). Furthermore, while this particular reaction

system is suitable for a mechanism study, it is not practical for use in the biomass industry. Therefore, an alternative is to introduce a catalyst so that the reaction can proceed at lower temperatures.
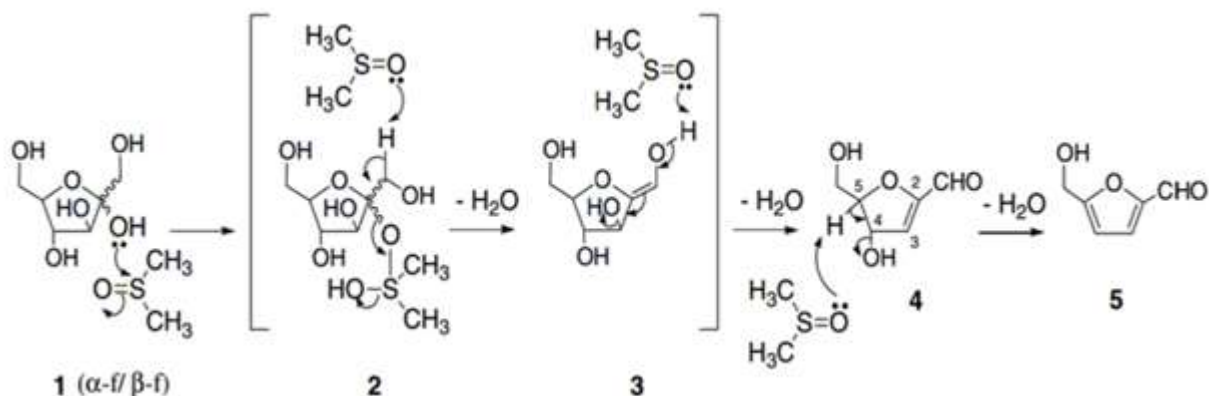
Scheme 2.5: Production of HMF using DMSO as catalyst (Amarasekara et al., 2008).
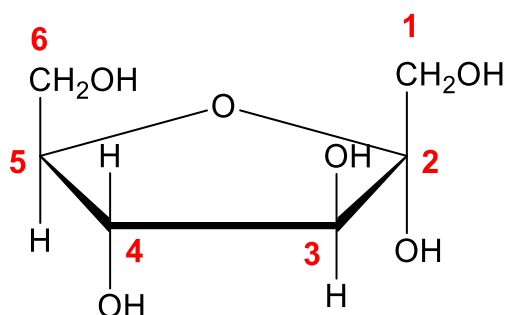
Figure 2.4: The carbon numbering in fructose.

Up to now, the research has tended to focus on the system of ILs and DMSO. An impressive 95.6 % conversion rate of fructose and 95.5 % HMF yield have been achieved in the presence of the dicationic ILs 1,1'-hexane-1,6-diylbis(3-methylpyridinium) tetrachloronickelate (II) ($[C_6(Mpy)_2]$ $[NiCl_4]^{2-}$) and DMSO under relatively mild conditions at 110 °C for 60 min (Jadhav et al., 2013). This study aimed to identify a suitable catalyst and DMSO system, and also provided a better understanding of the mechanism of HMF production.

CHAPTER 3: MATERIALS AND METHODOLOGY

3.1 Materials

α,α-dichloro-para-xylene (98 %), α,α-dichloro-ortho-xylene (98 %), α,α-dichloro-meta-xylene (98 %), benzyl-imidazole (99 %), 5-hydroxymethylfurfural (food grade, ≥ 99 %), DMSO (99 %) were purchased from Sigma Aldrich (St. Louis, Missouri, USA) and were used without further purification. Acetonitrile (HPLC grade) and methanol (HPLC grade) were purchased from Merck. DMSO (99 %), ethyl acetate (analytical grade), ethyl ether (analytical grade) and concentrated H_2SO_4 (≥ 98 %) were purchased from R&M chemicals (Essex, United Kingdom). D-fructose (USP grade, 98 to 102 %) was purchased from Fischer Scientific (Waltham, USA).

3.2 Synthesis of new ionic liquids

In this work, six new ILs were designed based on two different anions; chloride and hydrogen sulphate. As illustrated in **Table 3.1**, the uniqueness of these ILs can be seen through three different positions of benzyl imidazolium at ortho, meta and para in cationic site. These new ILs were prepared using two steps; alkylation and metathesis reactions.

Table 3.1: Six new ILs and their abbreviation.
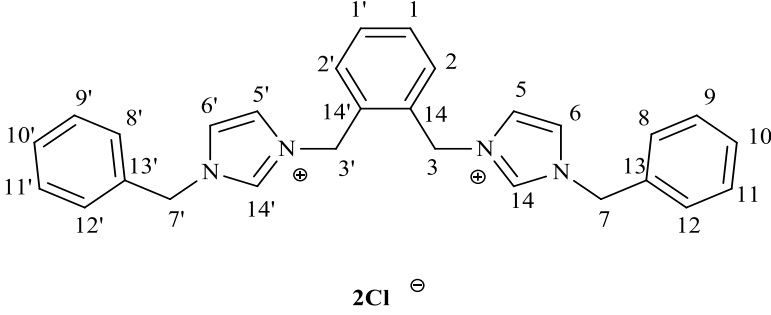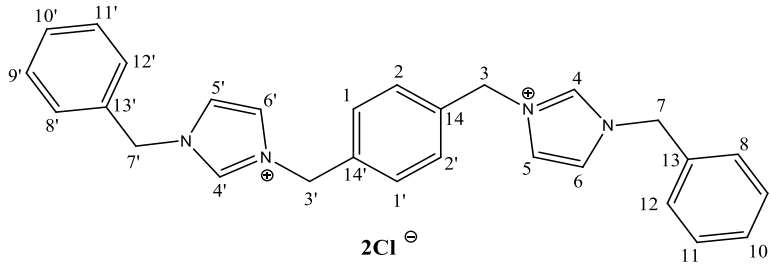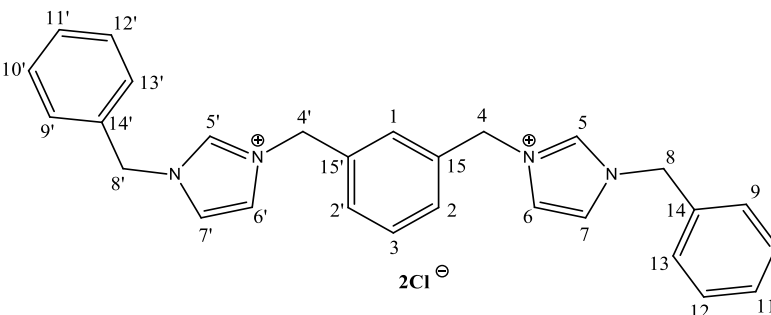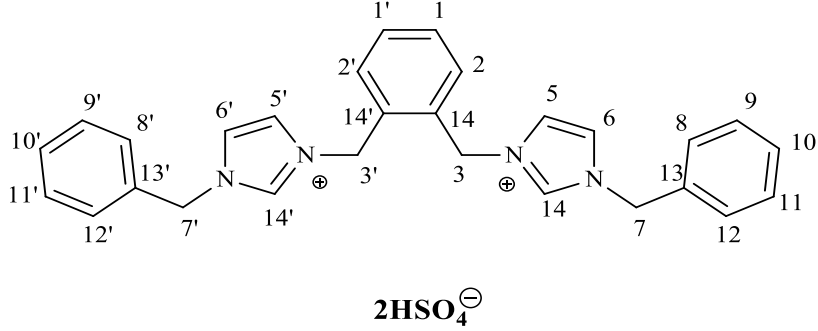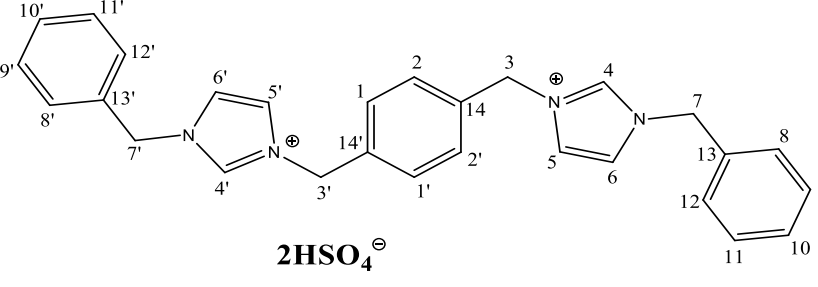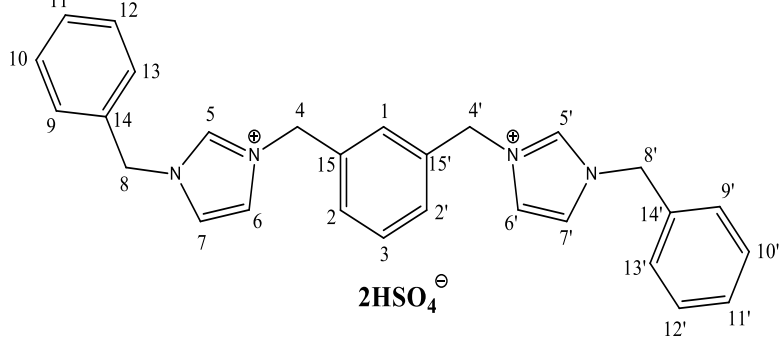
No	Structure	Abbreviation
1	3,3'-(1,2-phenylenebis(methylene))bis(1-benzyl-1H-imidazol-3-ium) dichloride	A-orthoCl
2	3,3'-(1,4-phenylenebis(methylene))bis(1-benzyl-1H-imidazol-3-ium) dichloride	B-paraCl
3	3,3'-(1,2-phenylenebis(methylene))bis(1-benzyl-1H-imidazol-3-ium) dichloride	C-metaCl

Table 3.1, continued

4		A-orthoHSO$_4$
	2HSO$_4^{\ominus}$	
	3,3'-(1,2-phenylenebis(methylene))bis(1-benzyl-1H-imidazol-3-ium) hydrogen sulfate	
5		B-paraHSO$_4$
	2HSO$_4^{\ominus}$	
	3,3'-(1,4-phenylenebis(methylene))bis(1-benzyl-1H-imidazol-3-ium) hydrogen sulfate	
6		C-metaHSO$_4$
	2HSO$_4^{\ominus}$	
	3,3'-(1,3-phenylenebis(methylene))bis(1-benzyl-1H-imidazol-3-ium) hydrogen sulfate	

3.2.1 Preparation of A-orthoCl, B-paraCl, C-metaCl through alkylation

Scheme 3.1 illustrates the synthesis routes for the **A-orthoCl, B-paraCl, C-metaCl** ILs by using benzyl-imidazole and three different positions of dichloro xylene known as α,α-dichloro-ortho-xylene, α,α-dichloro-meta-xylene and α,α-dichloro-para-xylene. Cl counter ion is chosen for the facile preparation of imidazolium based ILs. Dichloro-o-xylene or dichloro-p-xylene or dichloro-m-xylene (2.801 g, 0.0016 mol) and benzyl-imidazolium (5.206 g, 0.033 mol) were dissolved in 10 mL acetonitrile (ACN) and stirred at room temperature for 1 hour. Then, the mixture was heated under reflux for 18 hours at 80 °C. Then, two separated layer were obtained. The upper organic layer phase was decanted and the ILs layer was washed with ethyl acetate three times. The desired ILs with remaining trace of ethyl acetate and water was removed in a rotary evaporator and further dried in high vacuum for 2 hours to give > 90 % yield.

3.2.2 Preparation of A-orthoHSO₄, B-paraHSO₄, C-metaHSO₄ through metathesis

Scheme 3.2 illustrates the anion exchange by metathesis to produce **A-orthoHSO₄, B-paraHSO₄** and **C-metaHSO₄**. Generally, the metathesis reaction is facile as the cations from Cl based ILs formed more stable compound with HSO_4^-. The intention for this reaction is to obtain another set of isomeric dicationic ILs that have high acidity property while retains the hydrophilicity property. (6.416 g, 0.1 mol) of A-orthoCl, or B-paraCl or C-metaCl was added to 10 mL AcN and stirred at 0 °C for 10 minutes. Then, a stoichiometric amount of concentration H_2SO_4 was added drop wise and stirred for 1 hour at 0 °C and stirred for 15 hours at room temperature (25-28 °C). Next, continued with stirring for 4 hours at 60 °C. After completion reaction, the resultant ILs were washed with diethyl-ether and dried using vacuum pump for 2 hours at 80 °C.
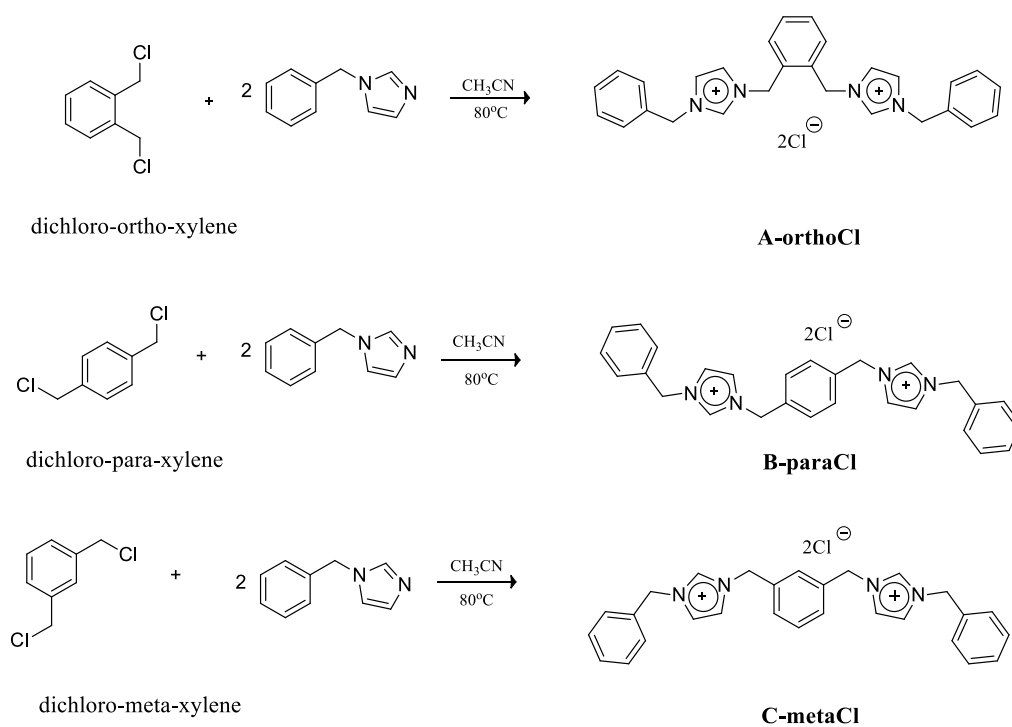
Scheme 3.1: Synthesis of dicationic ionic liquids.
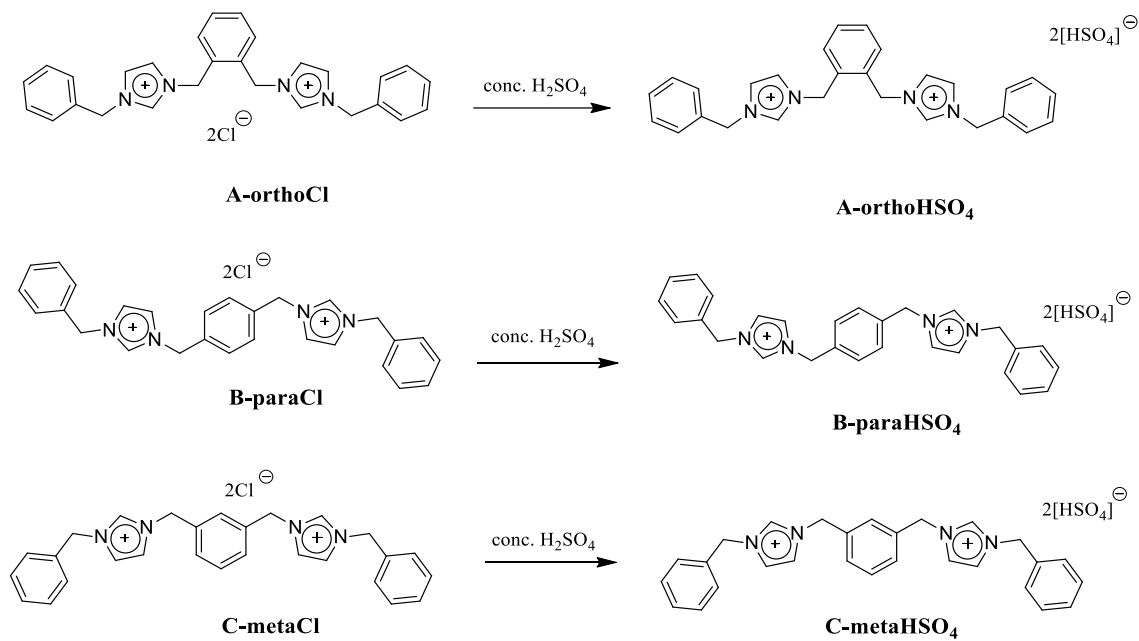
Scheme 3.2: Metathesis reaction.

.

3.3 Characterization of synthesized ILs

3.3.1 Fourier Transform Infrared spectroscopy (FTIR)

FT-IR experiment was conducted in the range of 4000-400 cm^{-1} by using sampling technique of attenuated total reflection (ATR) for the ILs analysis. It was performed on a Perkin-Elmer RX1 FT-IR spectrometer, (Massachusetts, US).

3.3.2 1H-NMR and 13C-NMR spectra

^{1}H-NMR and (400MHz) ^{13}C-NMR (100MHz) spectra were recorded using JEOL 400 FT-NMR, (Tokyo, Japan) spectrometer with chemical shifts relative to tetramethylsilane (TMS) as internal reference. DMSO-D$_6$ was used as solvent in all experiments.

3.3.3 Elemental analyses (CHN)

Elemental analyses of carbon, hydrogen and nitrogen were carried out by Perkin-Elmer 2400 Series II Elemental Analyser (Massachusetts, US). Samples were weight between 1.50 to 2.00 mg.

3.3.4 Thermal Gravimetric Analysis (TGA)

An inert static of nitrogen gas was used while conducting thermal gravimetric analysis by using Perkin Elmer TGA4000, (Waltham, USA). Temperature used was set from 40 to 700 °C at rate 10 °C/min.

3.3.5 Differential Scanning Calorimeter (DSC)

The phase transitions of synthesized ILs were determined by Differential Scanning Calorimeter, TA instrument DSC Q20 (New Castle, UK). Temperature used was set from 40 to 350 °C at rate 10 °C/min. An inert static of nitrogen gas was used in this experiment.

3.3.6 X-ray crystallography

Single crystal X-ray diffraction data for B-paraCl was collected at 296 K on Bruker AXS SMART APEXII, (Madison,USA) diffractometer with a CCD area detector ($\lambda_{MoK\alpha}=$ 0.71073 Å, monochromator = graphite). High quality crystal was chosen under the polarizing microscope and had been mounted on a glass fiber. Then, data processing and absorption correction was accomplished by using the APEXII software package.

3.3.7 Dynamic Light Scattering (DLS)

The zeta potential was measured at 25 °C by dynamic light scattering (DLS) using Malvern Zetasizer Nano (ZS) instruments, (Malvern, UK) and dichloromethane (DCM) was used as solvent to disperse the sample.

3.3.8 Acidity measurement using Hammett acidity function

The acidity of six ILs were evaluated from the determination of the Hammett functions (H_o) by UV-visible spectroscopy (UV-160A spectrometer, Shimadzu, Japan). Standard solutions of ILs (200 mmol/ L) and p-nitroaniline (0.2 mmol/L) in water were prepared and the experiment was conducted at 25°C both in the absence (1.5 mL of p-nitroaniline solution mixed with 1.5 mL water) and in the presence of the IL (1.5 mL of p-nitroaniline solution mixed with 1.5 mL water). The values of H_o have been calculated based on the intrinsic pKa of the indicator (p-nitroaniline) in water and the molar ratio of protonated and unprotonated dye [I]/[IH$^+$] using the following equation;

$$H_o = pK(I)_a + \log([I]/[IH^+]) \qquad (Eq.\ 3.1)$$

3.3.9 Solubility test

Approximately 0.10 g of each ILs was weight in a small vial. Then, 5 mL of selected solvents (H_2O, MeOH, DMSO, DMF, hexane, diethyl-ether and ethyl acetate) was added and shake vigorously.

3.4 Conversion of fructose to HMF

3.4.1 Dehydration reaction

The catalytic conversion of fructose to HMF was carried out in a round bottom flask with a condenser that was heated in an oil-bath. Before the reaction was started, the oil bath was preheated to 100 °C. D-fructose (1.00 g, 5.55 mmol) was dissolved in DMSO 10 mL, followed by the addition of the ILs catalyst (0.20 g). The temperature was varied from 40 to 160 °C. The reaction time was set from 30 min to 180 min and the catalyst loading from 0.01 g to 1.00 g.

3.4.2 Recyclability procedure

After the dehydration process, the reaction mixture was transferred into a conical flask. Then, 30 mL of distilled water was added to the mixture. The organic layer was extracted with ethyl-acetate (20 mL x 5) and distilled under reduced pressure to get pure HMF. The obtained HMF was then analyzed using ^{1}H-NMR. The remaining aqueous layer that contains ILs and DMSO was distilled under reduced pressure to get rid of water for 30 min and being used again in next reaction cycle. **Figure 3.1** presents the flow chart of the separation procedure.
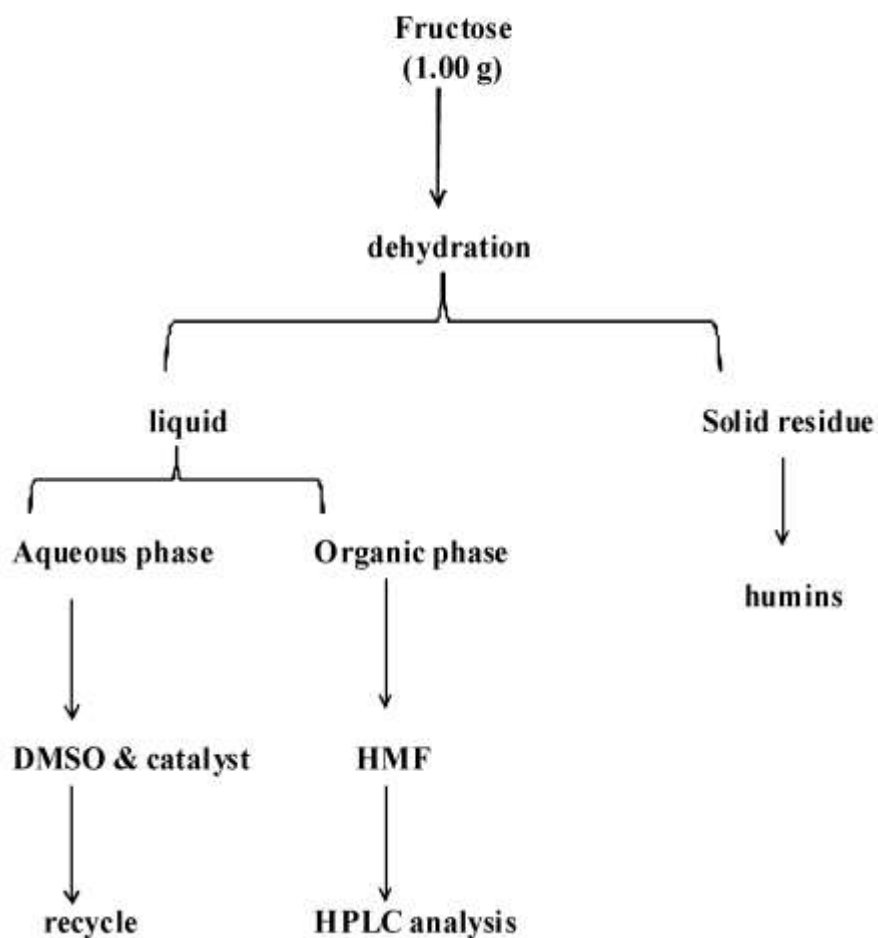
Figure 3.1: Separation procedure after the dehydration reaction.

3.5 HMF analysis

3.5.1 Preparation of standard solution of HMF

The stock solution of HMF was prepared in ultrapure water with concentration of 1000 mg/L. Next, the standard solutions containing 0.10, 0.15, 0.20, 0.50 mg/L of HMF were prepared freshly.

3.5.2 Sample preparation

20 μL solution from dehydration reaction was diluted into 10 mL centrifuge tube. Then, the existent of suspension was filtered out. While the supernatant was collected and filtered through 0.45 μm Milipore membrane and the filtrate was collected as sample solution.

3.5.3 HPLC-DAD instrumentation and chromatographic conditions

The amount of HMF in the dehydration reaction was calculated using an external standard at 25°C, analyzed through a HPLC apparatus equipped with C18 reverse column (250 mm x 4.6 mm, particle size 5 μm) hypersil gold, Thermo Science USA, SPD-M20A diode array detector, SIL-20AHT auto sampler and CTO-10ASVP column oven. The mobile phase was a mixture of methanol and water (40:60 v/v). The flow rate was set at 1.0 mL min^{-1}, and detection wavelength was at 283 nm. Then, analysis was conducted by using standard curve method. The calculation was presented as below:

   a) Mass HMF was calculated as follows,

$$\text{Mass HMF (mg)} = \text{HMF concentration} \left(\frac{\text{mg}}{\text{mL}}\right) \text{x Vol}_{RM} \text{ x DF} \qquad \text{(Eq. 3.2)}$$

In which,

Vol$_{RM}$ is the volume of reaction mixture = 10 mL

DF is dilution factor in dilution = (10 mL/0.02 mL) = 500

   b) The yield of HMF was calculated from equation,

$$\text{HMF yield (\%)} = \left(\frac{\text{moles of HMF formed}}{\text{initial moles of fructose}}\right) \text{X 100 \%} \qquad \text{(Eq. 3.3)}$$

$$= \left(\frac{\frac{M_{HMF\,(mg)}}{MW_{HMF}}}{\frac{M_{fructose\,(mg)}}{MW_{fructose}}}\right) \times 100\,\%$$

In which,

M $_{HMF}$ is the mass of HMF

M$_{fructose}$ is the mass of fructose

3.6 Fructose analysis

3.6.1 Preparation of standard solution of fructose

Stock solutions of fructose were prepared using ultrapure water with concentration of 1000 mg/L. Next, standard solutions containing 0.01, 0.02, 0.10, 0.25, 0.50 mg/L of fructose solution were prepared freshly.

3.6.2 Sample preparation

20 μL solution from dehydration reaction was diluted into 10 mL centrifuge tube. Then, the existent of suspension was filtered out. While the supernatant was collected and filtered through 0.45μm Milipore membrane and the filtrate was collected as sample solution.

3.6.3 HPLC-ELSD instrumentation and chromatographic conditions

HPLC analysis was performed on a Waters 2424 system. Separation was achieved on Phenomenex Luna 5u NH_2 100A column (250 mm x 4.60 mm, 5 μm). The mobile phase was consisted of acetonitrile: water ratio (80:20, v/v) was degassed by ultrasonic bath prior to use. Each run was completed within 10 min. The drift tube temperature and nitrogen gas flow were set up at 80 °C and 2 L/min respectively. The flow rate was 1 mL/min and an aliquot of 20 μL of sample solution was injected into HPLC-ELSD system. All samples and standard were filtered through 0.45μm Milipore membrane before used. Fructose conversion was calculated as below.

$$\text{conversion \%} = \left(1 - \frac{\text{Fructose conc.in the product}}{\text{Fructose conc. in the loaded sample}} \right) \text{x } 100 \text{ \%} \qquad \text{(Eq.3.4)}$$

In this experiment also, product selectivity was calculated by using equation as below,

$$\text{selectivity \%} = \frac{\text{Yield of product}}{\text{Fructose conversion}} \qquad (\text{ Eq.3.5})$$

3.7 In situ NMR study

In situ NMR was conducted to study the selectivity of highest catalytic activity ILs (A-orthoHSO$_4$) in HMF production and further understanding the reaction mechanism. In this experiment, a solution of D-fructose (25 mg) and (17.5 mg) of the A-orthoHSO$_4$ in 0.5 mL of DMSO-d$_6$ was prepared in a NMR tube. The tube was then transferred to NMR spectrometer. ^{1}H-NMR spectra were recorded at room temperature (23.0 °C). Then, the ^{1}H-NMR spectra were recorded at 5 min, 20 min, 40 min and 60 min of reaction while keeping the temperature constant at 100 °C.

CHAPTER 4: RESULTS AND DISCUSSION

4.1 Characterization of new dicationic liquids

Six new ILs have been successfully synthesized and characterized in this work. Their names and abbreviations are listed previously in **Table 3.1**. Structural elucidations were carried out using infra red (IR), nuclear magnetic resonance (NMR), elemental analyses of carbon, hydrogen, and nitrogen (CHN), and x-ray crystallography. Other important physical properties were evaluated via thermal gravitational analysis (TGA), differential scanning calorimetry (DSC), and dynamic lightening scattering (DLS).

4.1.1 Fourier Transform Infrared spectroscopy analysis

FT-IR spectroscopy was used mainly to study the bonding activity of synthesized ILs. This spectroscopy analysis is one the prominent methods to identify the major difference between Cl^- and HSO_4^- based ILs, and significant vibrations corresponding to dicationic bonding. The results were recorded and crosschecked with a previous report (Matuszek et al., 2014).

The main IR vibration bands of all six ILs were found in their expected regions and are listed in **Table 4.1**. The characteristic peak of S-O stretching ν(S-O) between 841 and 851.97 cm^{-1} indicates the formation of A-orthoHSO$_4$, B-paraSO$_4$, and C-metaHSO$_4$. In addition, the existence of the HSO_4 anion was further confirmed by a weak band observed between 1347 and 1359 cm^{-1} attributed to ν(S-OH), due to strong hydrogen bonding between two HSO_4anion restricting the stretching motion (Matuszek et al., 2014; Yacovitch et al., 2011). A strong IR peak was observed between 1000 and 1142 cm^{-1} corresponding to S=O stretching.

Table 4.1: Vibrations frequency in the FT-IR spectra.

Compound	Wavenumber, ν (cm^{-1})					
	C=C aromatic	C=N	C-N	S-OH	S=O	S-O
A-orthoCl	1557.84, 1444.76	1630.60	1357.16	-	-	-
B-paraCl	1556.20, 1455.27	1649.85	1352.36	-	-	-
C-metaCl	1557.39, 1453.60	1661	1355.05	-	-	-
A-orthoHSO$_4$	1561.03, 1406.38	1643.02	1212.95	1359.12	1149.76, 1000.88	851.97
B-paraHSO$_4$	1555.42, 1451.21	1627.12	1233.95	1347.65	1142.62, 1025	841.84
C-metaHSO$_4$	1559.09, 1451.96	1613.84	1206.89	1349.35	1145.87, 1029.13	850.47

Table 4.1 shows the FT-IR spectra of Cl$^-$ and HSO$_4^-$ based ILs. These results evidence the success of anion substitution and metathesis reaction. Additionally, all important peaks (C=C, C=N, and C-N) were observed for both Cl$^-$ and HSO$_4^-$ based ILs.
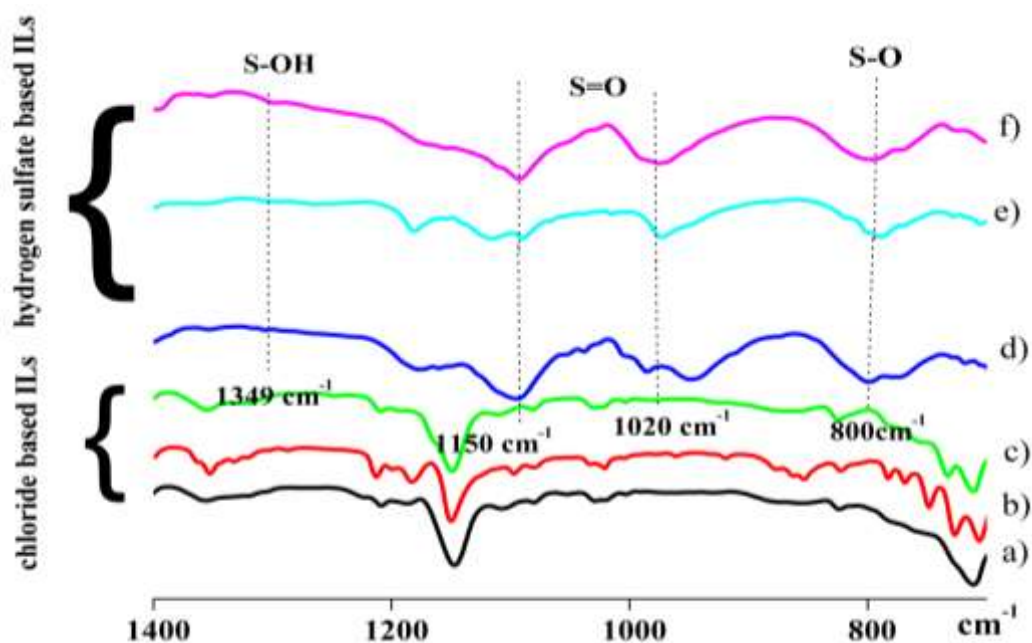
Figure 4.1: FT-IR spectra of chloride and hydrogen sulfate based ILs. a) A-orthoCl, b) B-paraCl, c) C-metaCl, d) A-orthoHSO$_4$, e) B-paraHSO$_4$, f) C-metaHSO$_4$.

4.1.2 Nuclear Magnetic Resonance (NMR) spectroscopy

4.1.2.1 ^{1}H-NMR

^{1}H-NMR was carried out to confirm the structure of the ILs. The characteristic patterns of each ILs molecule can be recognized by the difference in peak splitting for the ortho, meta, and para ILs also their chemical shifts. **Table 4.2** provides an overview of the ^{1}H-NMR results obtained.

Table 4.2: Chemical shift and multiplicity of six ILs.

Compound	Chemical shift, δ (ppm) and multiplicity
A-orthoCl	5.48ppm, 2H (H7), s; 5.74ppm, 2H (H3), s; 7.36-7.48ppm, 5H (H5,H6,H8,H9,H10), m; 7.52ppm, 2H (H1), d, J_{H-H}= 7.56 Hz; 7.60ppm, 2H (H2), d, J_{H-H}= 9.27 Hz; 9.77ppm, 1H (H4), s
B-paraCl	4.64ppm , 2H (H7), s; 4.67ppm , 2H (H3), s; 6.58-6.66ppm, 6H, (H5, H6, H8, H9, H10), m; 6.72ppm, 2H (H1), d, J_{H-H}= 0.92Hz; 6.86ppm,2H (H2), d, J_{H-H}=0.89Hz; 9.75ppm, 1H (H4), s
C-metaCl	5.34ppm, 2H (H8), s; 5.38ppm, 2H (H4), s; 7.13-7.26, 1H (H1), m; 7.27-7.42, 4H (H2,H9, H10, H11), m; 7.49-7.55, 1H (H3), m 7.58-7.62, 2H (H6, H7), m 10.14, 1H (H5), s.
A-orthoHSO$_4$	1.30ppm, 1H (OH from anion), s; 5.43ppm, 2H (H7), s; 5.65ppm, 2H, (H3), s; 7.38ppm, 1H (H1), dd, J_{H-H}=5.50Hz; 7.40-7.44ppm, 1H (H2),m; 7.44-7.50ppm, 3H (H8, H9, H10), m; 7.50-7.56ppm, 2H (H5, H6), m; 9.45ppm, 1H(H4) s.

Table 4.2, continued

B-paraHSO$_4$	1.87ppm, 1H, (OH from anion), s; 5.41ppm, 4H, (H3, H7), d; 7.30-7.43ppm, 3H, (H8, H9, H10), m; 7.44-7.48ppm, 2H, (H1, H2), m; 7.81ppm, 2H, (H5, H6), d; 9.48ppm, 1H, (H4), s
C-metaHSO$_4$	2.03ppm, 1H, (OH from anion), s; 5.38ppm, 2H, (H8), s; 5.42ppm, 2H, (H4), s; 7.37-7.41ppm, 1H, (H1),m; 7.44-7.50ppm,7H,(H2, H3,H6, H7, H9, H10, H11),m; 9.54ppm, 1H, (H5), s.

The chemical shift patterns of C2-H imidazolium (**Figure 4.2**) of ortho, meta, and para ILs with Cl$^-$ or HSO$_4^-$ anion, and their ^{1}H-NMR spectra are shown in **Figure 4.3**. The peaks corresponding to Cl based ILs are shifted downfield because the electronegative Cl anion shields the proton from the applied magnetic field. The behavior of C2-H is important in understanding the fundamental difference between the ortho, meta, and para ILs with respect to polarity, acidity and hydrogen bonding interaction in mechanism reaction (Noack et al., 2010).
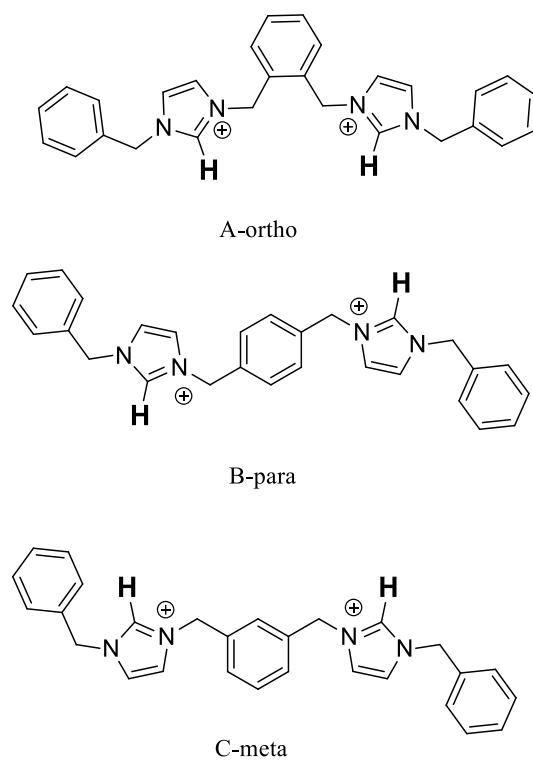
A-ortho

B-para

C-meta

Figure 4.2: C2-H imidazolium of A-ortho, B-para and C-meta.
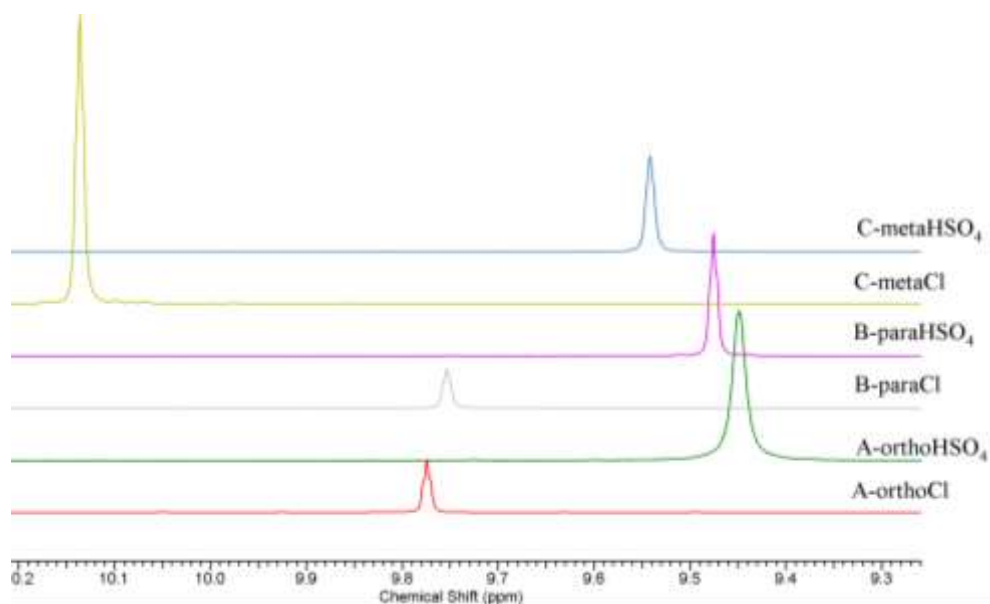
Figure 4.3: ^{1}HNMR spectra (400 MHz) of C2-H imidazolium for all six ILs.

Figure 4.4, 4.5, and **4.6** shows the 400 MHz ^{1}H-NMR spectra of Cl$^-$ and HSO$_4^-$ based ILs. It is apparent from **Figure 4.4** that the characteristic pattern of para di-substituent is easy to identify as both H1 and H2 have the same chemical shift due to them having a similar environment. Consequently, it gives a doublet signal at 7.86–7.87 ppm for Cl based anion and 7.78 ppm for HSO$_4$ anion.
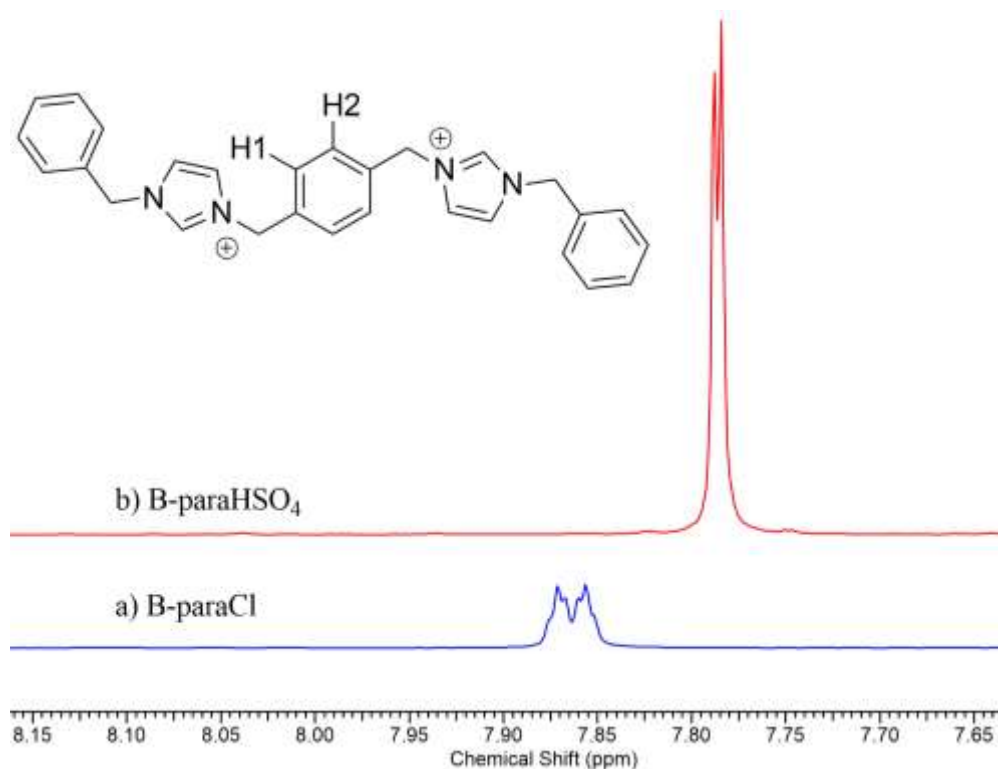
Figure 4.4: ^{1}H-NMR of a) B-paraCl and b) B-paraHSO$_4$ ILs.

On the other hand, ortho and meta ring substitution resulted in a more complicated splitting pattern (Pavia et al., 2010). In the case of ortho substitution, interaction of adjacent H produced a doublet signal for H2 at 7.83 ppm for Cl$^-$ and 7.70-7.76 ppm for HSO$_4^-$. Additionally, a multiplet signal representing H1 was recorded at 7.41-7.46 ppm for HSO$_4^-$ and 7.45-7.47 ppm for Cl$^-$. **Figure 4.5** shows the shift difference in both ILs anions.
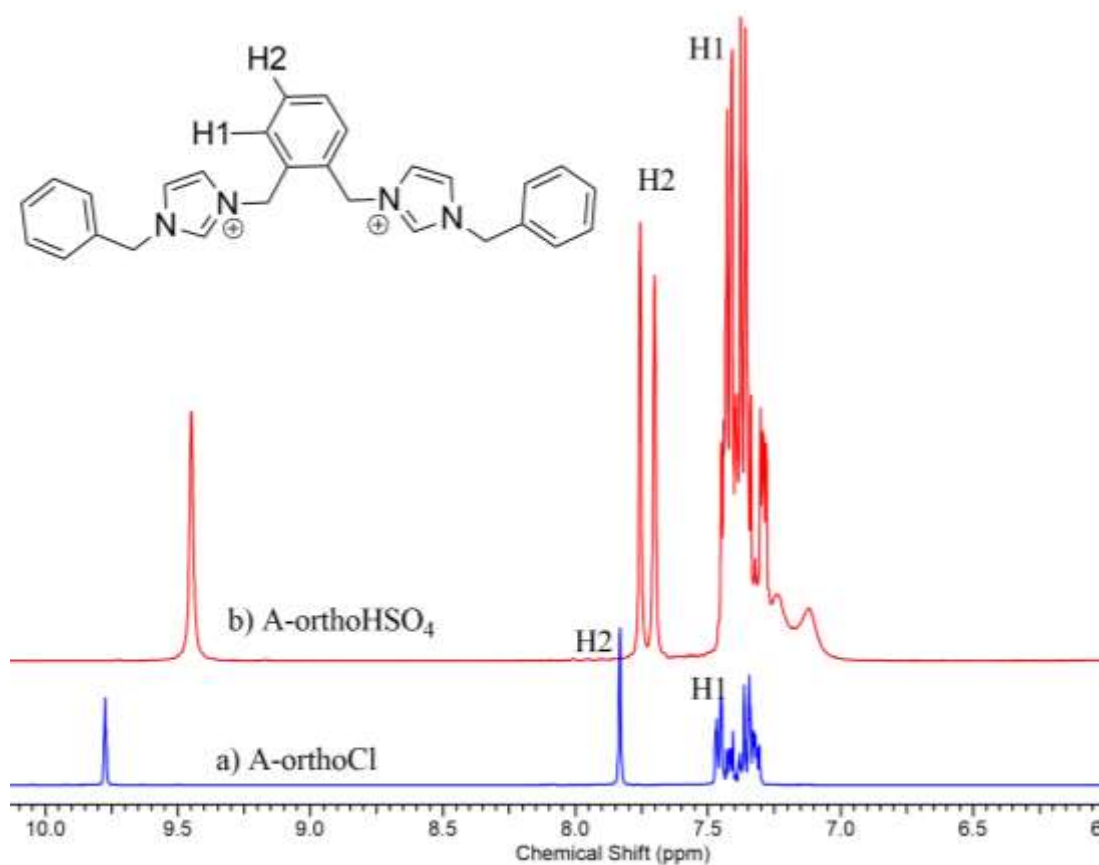
Figure 4.5: ^{1}H-NMR of A-orthoCl and A-orthoHSO$_4$ ILs.

Meanwhile, examination on the ^{1}H-NMR spectrum of C-meta revealed three different splitting patterns of H1 (singlet), H2 (doublet of triplet) and H3 (triplet). **Figure 4.6** shows the fingerprints of C-meta compounds and their detailed shift values are tabulated in **Table 4.2**. The spectrum also shows a multiplet pattern between 7.30 and 7.50 ppm corresponding to the terminal benzene group.
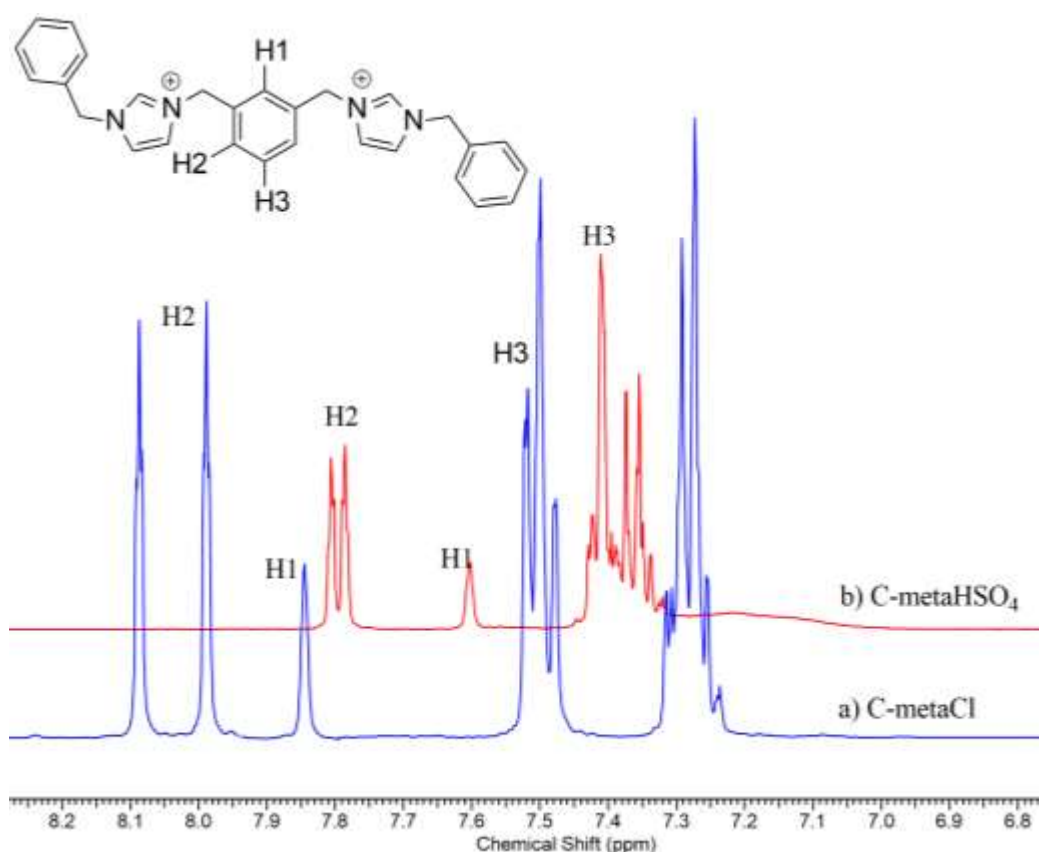
Figure 4.6: ^{1}H-NMR of a) C-metaCl and b) C-metaHSO$_4$ ILs

The difference between Cl$^-$ and HSO$_4^-$ based ILs is in its shifting pattern. It is clearly shown in **Table 4.2** that the splitting of Cl$^-$ based ILs were shifted to higher frequencies than for the HSO$_4$ based ILs. This means that the hydrogen have a different environment to resonance. These results evidence the success of the metathesis reaction.

4.1.2.2 ^{13}C-NMR

All carbon signals that correspond to carbon elements in the ILs are listed in **Table 4.3**. The most upfield signal was assigned to C3 and C7 (A-ortho and B-para), and C4 and C8 (C-meta) of the methylene groups. The peaks that appeared in the range of 136.46 to 145.67 ppm were assigned to carbon C4 (A-ortho) and C5 (C-meta) belonging to the imidazolium ring of ILs.

Table 4.3: Chemical shift and multiplicity of six ILs.

Compound	Chemical shift, δ (ppm)
A-orthoCl	49.97 ppm (C7); 53.00 ppm (C3); 122.69 ppm (C5,C6); 122.91 ppm (C1); 128.77 ppm (C10); 129.19 ppm (C8); 129.24 ppm (C2); 130.37 ppm (C9); 132.29 ppm (C13); 133.96 ppm (C14); 136.46 ppm (C4)
B-paraCl	53.33 ppm (C7); 53.96 ppm (C3); 123.85 ppm (C6); 123.87 ppm (C5); 128.48 ppm (C1); 129.44 ppm (C10); 130.11 ppm (C8); 130.16 ppm (C2); 130.41 ppm (C9); 134.94 ppm (C13); 136.13 ppm (C14); 137.30 ppm(C4)
C-metaCl	52.29 ppm (C8); 52.80 ppm (C4); 122.69 ppm (C7); 122.79 ppm (C6); 128.56 ppm(C1); 129.00 ppm (C10); 129.08 ppm(C9); 129.31 ppm (C2); 130.10 ppm (C11); 133.98 ppm(C3); 135.19 ppm (C14); 135.21 ppm (C15); 136.12 ppm (C5)
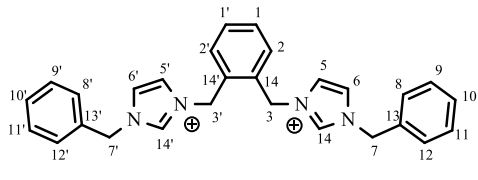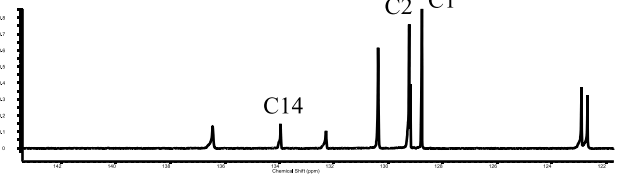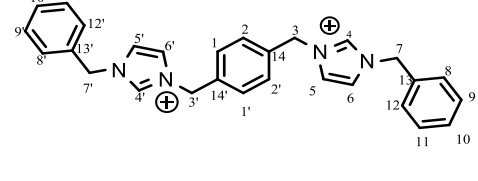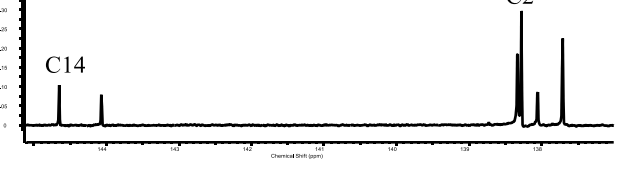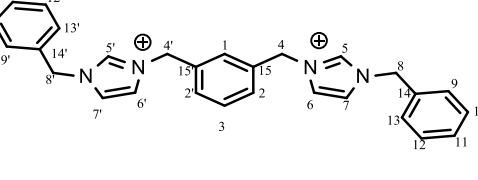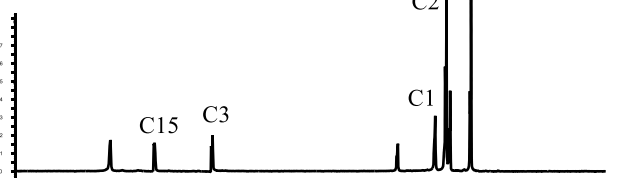
Table 4.3, continued

A-orthoHSO$_4$	51.01ppm (C7); 54.11ppm (C3); 123.79 ppm (C6); 124.05 ppm (C5); 129.87 ppm (C1); 130.25 ppm (C10); 130.31 ppm (C8); 131.42 ppm (C2); 131.47 ppm (C9); 133.51 ppm (C13); 135.15 ppm (C14); 137.74 ppm (C4)
B-paraHSO$_4$	60.79 ppm (C7); 61.27 ppm (C3); 132.14 ppm (C5,C6); 132.18 ppm (C1); 137.71 ppm (C10); 138.05 ppm(C8); 138.28 ppm (C2); 138.33 ppm (C9); 144.07 ppm (C13); 144.65 ppm (C14); 145.67 ppm (C4)
C-metaHSO$_4$	53.37 ppm (C8); 53.49 ppm (C4); 123.75 ppm (C6,C7); 123.88 ppm (C1); 129.57 ppm (C10); 129.71 ppm (C9); 130.16 ppm (C2); 130.31 ppm (C11); 130.43 ppm (C3); 135.16 ppm (C14); 136.36 ppm(C15); 137.25 ppm (C5)

The most interesting aspect of ^{13}C-NMR study is to identify the distinctive different of

the ILs isomers. **Table 4.3** shows that the aromatic carbons exhibit resonance in the range

of 122.91 to 144.65 ppm. These aromatic molecules exhibit unique signals corresponding

to their di-substituted ortho, meta, and para forms. In fact, planes of symmetry in the A-

ortho, B-para and C-meta ILs resulted in a lower number of carbon peaks. **Table 4.4** presents the three different patterns that allow the A-orthoCl, C-metaCl and B-paraCl substituent to be distinguished. A symmetrical di-substituted benzene ring produced three unique carbon signals for ortho (C1, C2 and C14), four unique carbon signals for meta (C1, C2, C3, C15) and two unique carbon signals for para (C2 and C14) (Pavia et al., 2010). The remaining peaks are due to the terminal benzene molecules.

Table 4.4: The unique characteristics of ^{13}C-NMR for a) A-orthoCl, b) B-paraCl and c) C-metaCl ILs.

4.1.3 Elemental analyses

Experimental and theoretical values of carbon, hydrogen and nitrogen content in the six new ILs are tabulated in **Table 4.5**. The purity of the prepared compounds and the percentage of C, H and N are given based on the direct weight of the sample.

However, it is apparent from the data that the experimental results deviated slightly from the theoretical value calculated. This might be due to the excessive moisture in the ILs and incomplete combustion during elemental analysis. The result also shows the significant difference in the C, H and N content between Cl^- and HSO_4^-based ILs. The errors between calculated and theoretical values are small, being between 0.13 to 2.7 %. Therefore the CHN results are valid and support the proposed composition of synthesis ILs.

Table 4.5: Carbon, nitrogen and hydrogen analyses of the six new dicationic ILs.

ILs	Molecular formula	Data	C%	H%	N%
A-orthoCl	$C_{28}H_{28}C_{l2}N_4$	Theoretical	68.430	5.740	11.400
		Experimental	67.337	5.867	11.698
B-paraCl	$C_{28}H_{28}C_{l2}N_4$	Theoretical	68.430	5.740	11.400
		Experimental	69.630	5.918	12.012
C-metaCl	$C_{28}H_{28}C_{l2}N_4$	Theoretical	68.430	5.740	11.400
		Experimental	67.862	6.267	12.698
A-orthoHSO$_4$	$C_{28}H_{30}N_4O_8S_2$	Theoretical	54.710	4.920	9.110
		Experimental	55.062	2.267	10.198
B-paraHSO$_4$	$C_{28}H_{30}N_4O_8S_2$	Theoretical	54.710	4.920	9.110
		Experimental	53.962	5.160	10.971
C-metaHSO$_4$	$C_{28}H_{30}N_4O_8S_2$	Theoretical	54.710	4.920	9.110
		Experimental	55.902	5.407	10.008

4.1.4 Thermal analysis

Thermogravimetric analysis (TGA) was used to investigate the decomposition behavior of ILs. The results are shown in **Figure 4.7**. For some of the ILs, the weight loss below 100 °C is due to the volatilization of residual water or organic solvent that was

used during the separation step. At higher temperatures of 250-300 °C, a second stage of weight loss can be observed. At this stage, all six ILs underwent thermal degradation with a total mass loss in the range of ~65-75 wt % due to the degradation of benzyl group (Erdmenger et al., 2008). The detailed TGA analysis was tabulated on **Table 4.6**. It was also observed that the Cl^- based ILs decomposed in the range of 14.80 to 46.43°C lower than HSO_4^- based ILs. It is believed that, the more hydrophilic the ILs, the lower the thermal stability (Huddleston et al., 2001).

It was also found that HSO_4^- successfully increased the thermal stability of the ILs because of its higher molecular weight. In addition, the inter- and intra- molecular forces such as hydrogen bonding interaction among the molecules also contributed to its stability. It can be concluded that the anion plays a more significant role compared to the cation. Therefore, a simple alteration of anion can be carried out in order to achieve a highly stable ILs. This result is in good agreement with a report by (Huddleston et al., 2001; S. Zhang et al., 2005).
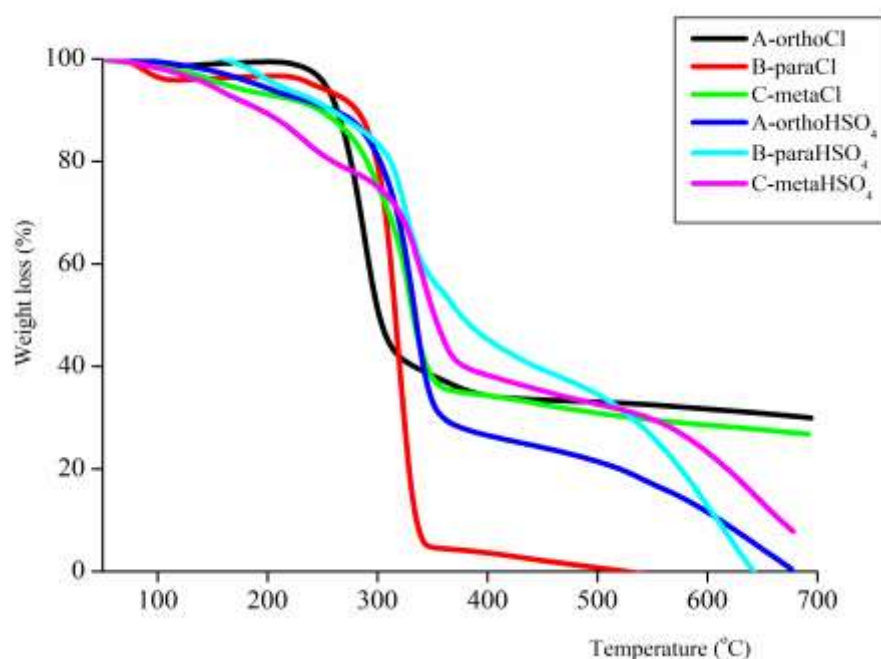
Figure 4.7: Thermogravimetric analysis of six ILs.

The thermal behaviour of ILs was further investigated using differential scanning calorimeter (DSC). **Figure 4.8, 4.9,** and **4.10** compared the DSC results of Cl^- and HSO_4^- based ILs. The behavior of each IL is relatively interesting as it reveals their phase change and specific thermophysical properties that can be utilized in future applications. In general, the unique properties of ILs are due to the structural variation caused by the cation or both cation and anion. A comparative study was conducted focusing on the difference in phase behavior for the cationic isomers and the anionic effects.

Table 4.6: TGA analysis of six ILs.

ILs	Temperature (°C)		Percentage loss		Assignment	
A-orthoCl	I.	49.97 – 127.23	I.	2.78%	I.	Water or residue solvent.
	II.	212.10– 289.04	II.	58.17 %	II.	Imidazolium and benzyl group
B-paraCl	I.	50.01 -117.69	I.	4.85 %	I.	Water or residue solvent.
	II.	267.37- 319.92	II.	80.28 %	II.	Imidazolium and benzyl group.
C-metaCl	I.	50.24- 128.85	I.	0.81 %	I.	Water or residue solvent
	II.	220.19- 331.66	II.	57.30 %	II.	Imidazolium and benzyl group.
A-orthoHSO$_4$	I.	47.74-128.57	I.	3.55 %	I.	Water or residue solvent.
	II.	290.30-375.77	II.	65.14 %	II.	Imidazolium and benzyl group.
B-paraHSO$_4$	I.	48.07-114.18	I.	20.35 %	I.	Water and residue solvent.
	II.	236- 358.43	II.	47.34 %	II.	Imidazolium and benzyl group.
C-metaHSO$_4$	I.	50.04- 109.84	I.	0.87 %	I.	Water and residue solvent.
	II.	151- 384.18	II.	46.90 %	II.	Imidazolium and benzyl group
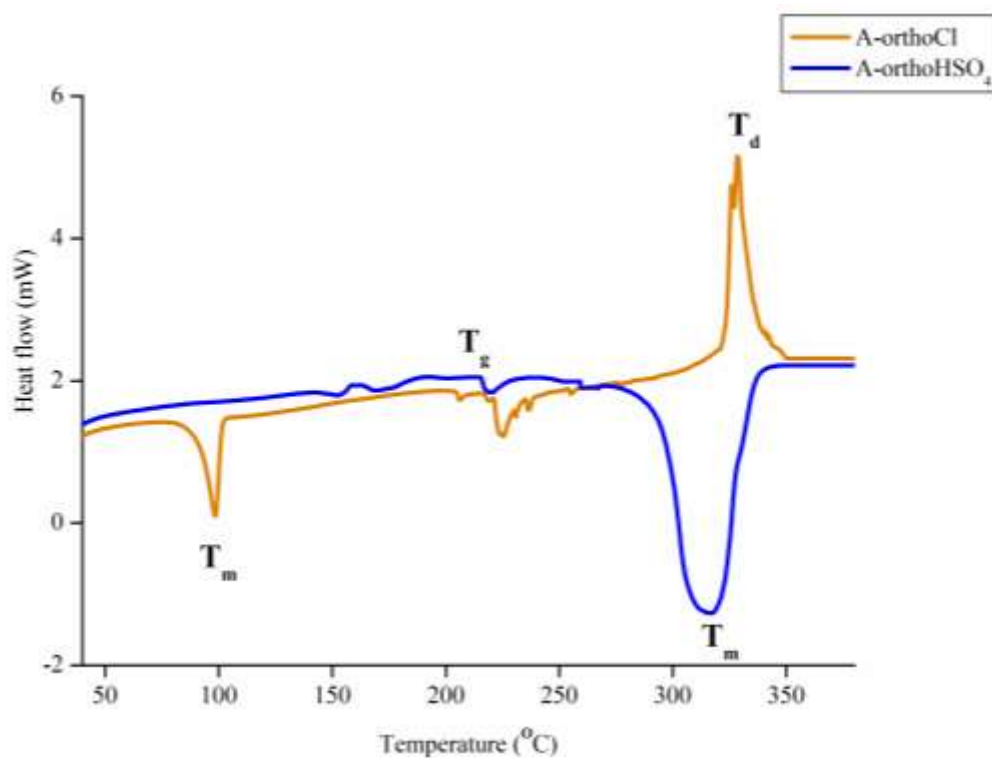
Figure 4.8: DSC thermogram of A-orthoCl and A-orthoHSO$_4$.
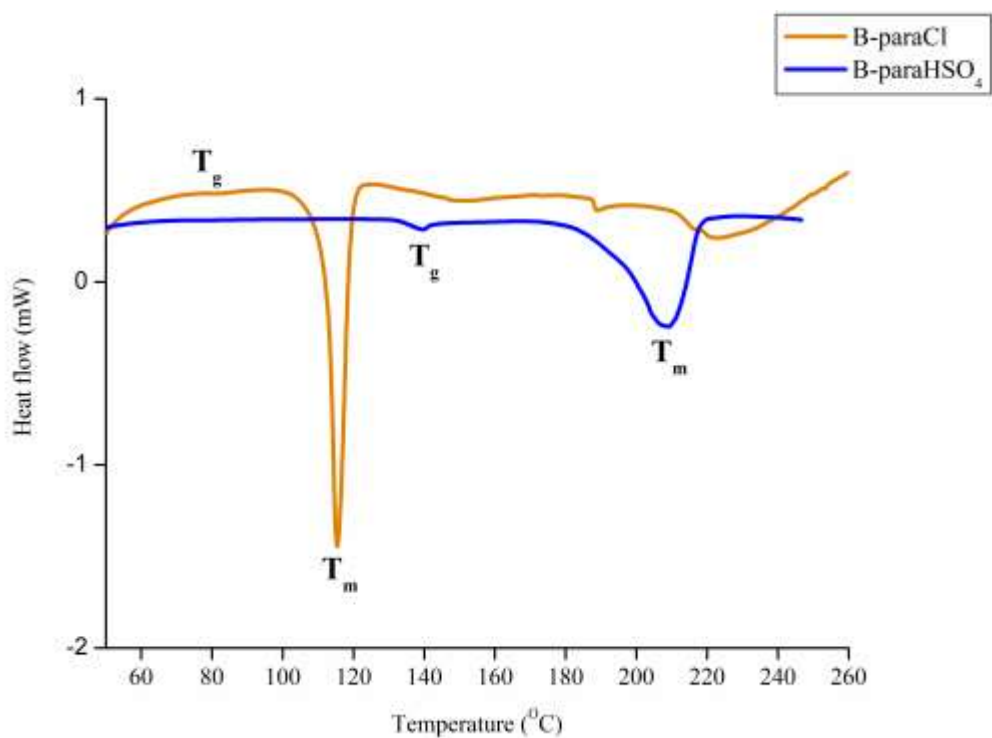
Figure 4. 9: DSC thermogram of B-paraCl and B-paraHSO$_4$.
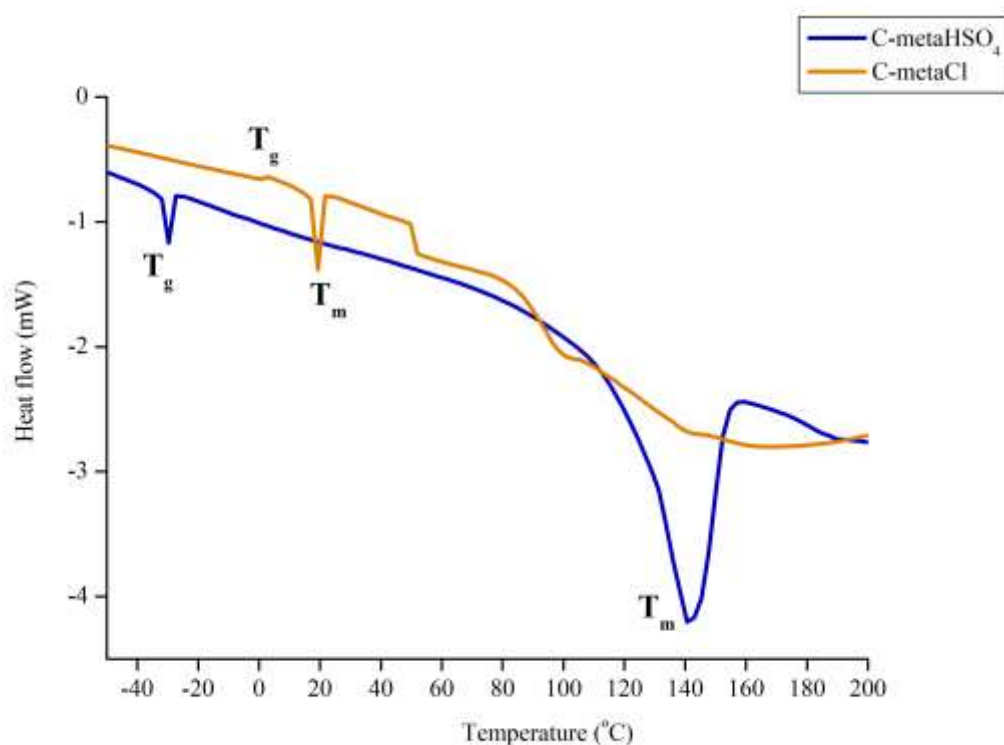
Figure 4. 10: DSC thermogram of C-metaCl and C-metaHSO$_4$.

During the heating scan, there are three important events that will occur. The first is the single glass transition at temperature T_g that usually occurs at the beginning of the scan. However, for the A-orthoCl, T_g was not observed likely because the phase transition was too small or it had happened at a lower temperature.

The second event is the melting process that occurs at T_m. As the temperature increases, a sharp peak in the thermogram is observed due to the endothermic nature of the melting process. Factors that influence T_m is related to the strength of the crystal lattice which itself is a function of intermolecular forces, molecular symmetry, and conformational degree of the molecules (Zhou et al., 2004). A noticeably higher T_m was observed for HSO$_4^-$based ILs compared to Cl$^-$ based ILs. This is due to the higher molecular weight of HSO$_4^-$ resulting in a more pronounced Van der Waals interaction in the salts.

Finally, the third event is the decomposition that occurs at temperature T_d. The T_d obtained from this analysis agrees with the decomposition temperature results obtained from TGA. **Table 4.7** summarizes the thermal phase of the six ILs.

Table 4. 7: Thermal characteristic of six ILs.

No	Ionic liquids	*Appearance at room temperature (28.0 °C)	T_g (°C)	T_m (°C)	T_d (°C)
1	A-orthoCl	White solid	-	98.47	289.04
2	B-paraCl	White solid	85.55	110.10	319.92
3	C-metaCl	Yellow viscous oil	17.69	22.42	331.66
4	A-orthoHSO$_4$	White solid	216.79	318.93	335.47
5	B-paraHSO$_4$	White solid	139.48	208.89	334.72
6	C-metaHSO$_4$	White waxy solid	-29.25	137.87	359.93

* Observation was recorded after two weeks of synthesized.

4.1.5 X-ray crystallography

All synthesized ILs were in the liquid state when they were freshly synthesized. However, after two weeks, the A-orthoCl and B-paraCl ILs solidified whereas the C-metaCl ILs became more viscous. This observation raises an important question regarding their crystallinity. Previous research (Choudhury et al., 2005; Mondal et al., 2014) suggested that it had occurred because of the nature of hydrogen bonding, anion disorder, and crystal packing. In this case, it can be understood that the transformation from liquid to solid or semi-solid state was triggered by the incorporation of water molecules stabilized by hydrogen bonding.

In this context also, it proved that the crystallization process occurred slowly at room temperature (28.0 °C) within two weeks. This phenomenon has been reported for other ILs in earlier works as well (Fredlake et al., 2004; Kotadia & Soni, 2013). The crystallinity properties of these ILs were further investigated by X-ray crystallography analysis. The reason that C-metaCl remained relatively unchanged is probably due to the geometry effect or coordinate orientation that caused the ILs packing to have a lower order of conformation (Fumino et al., 2008).

An investigation had been carried out to understand this solidification phenomenon. Single crystal of B-paraCl was able to grow at room temperature, 28.0 °C and the result was presented in **Figure 4.11**. This compound was crystallized in the P21/*c* space group with the monoclinic crystal system when methanol was used as a medium for crystal growth. Based on the ortep diagram, the single crystal allows for the better understanding of the covalent and ionic bonds and clarification of the structure of B-paraCl. Interestingly, it is revealed that H_2O crystal locking caused the solidification process to take place.
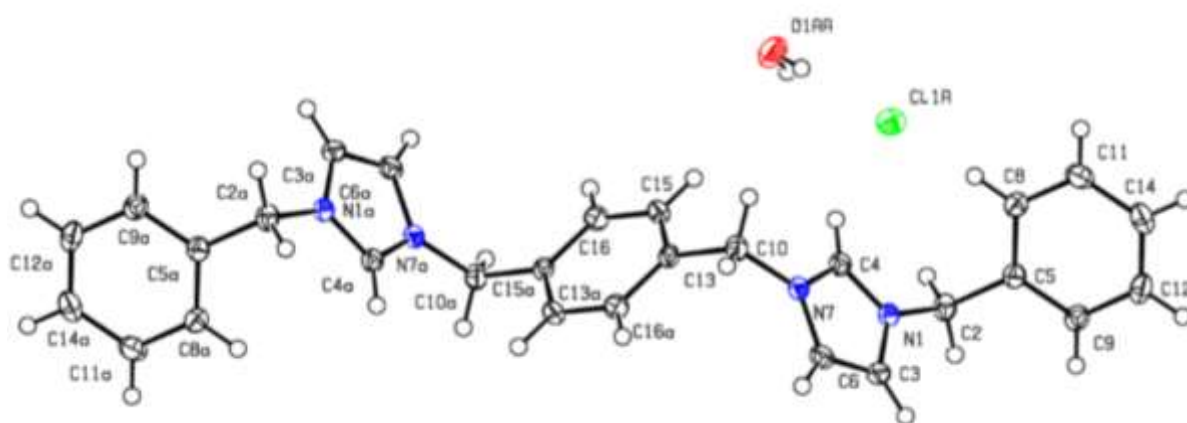
Figure 4. 11: Ortep diagram of B-paraCl

4.1.6 Size distribution by Dynamic Light Scattering (DLS)

The analyses of the particles size of ILs were conducted using dynamic light scattering (DLS). The measurement is based on the hydrodynamic diameter where it refers to the diameter of the particle, ligands, ions, or molecules that are associated with the surface and travel with the particle in solution.

According to the results demonstrated in **Figure 4.12** and **4.13**, the smallest molecular size was achieved by the HSO_4^- based ILs. The ILs with ortho position has high molecular size with 1295.92 nm followed by meta, 659.93 nm and para, 230.30 nm. However, the trend in Cl^- based ILs was vice-versa where the highest particle size was recorded for B-

para with 3842.45 nm followed by C-meta and A-ortho with 3083.94 nm and 888.16 nm, respectively. The sizes of A-ortho compound for both anions do not show much difference. Meanwhile, B-para and C-meta show dramatic changes of size where it becomes extremely small in HSO_4^- based anion, respectively.
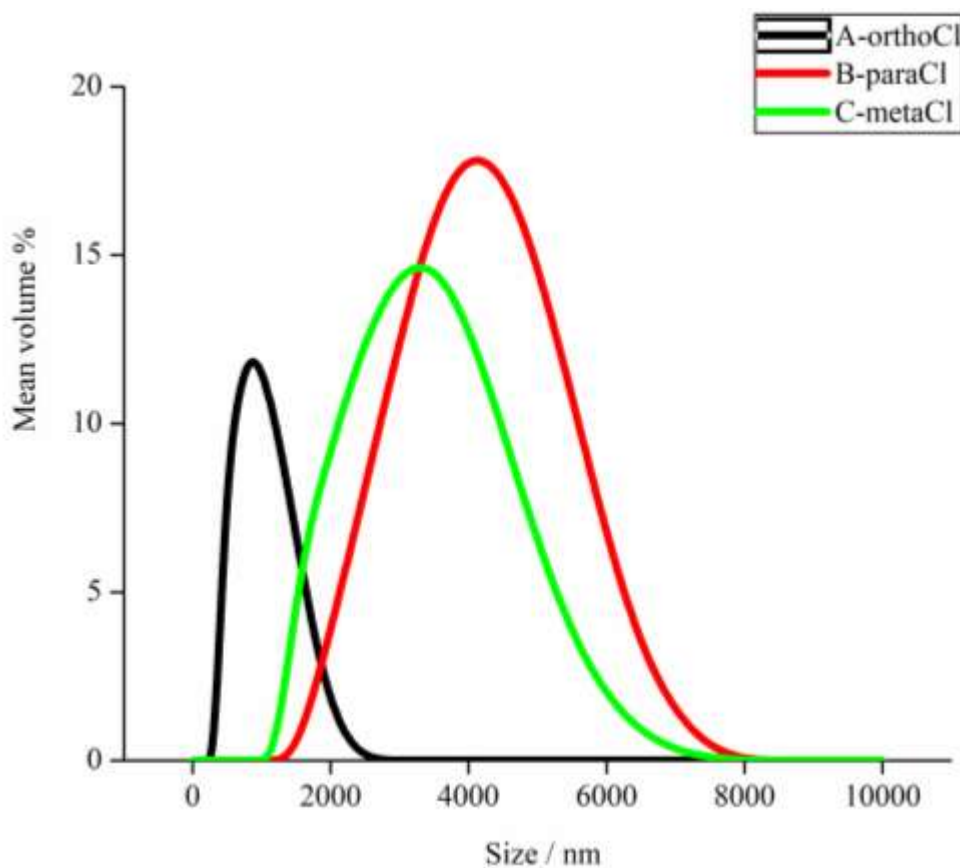
Figure 4.12: Size distribution of Cl based ILs.
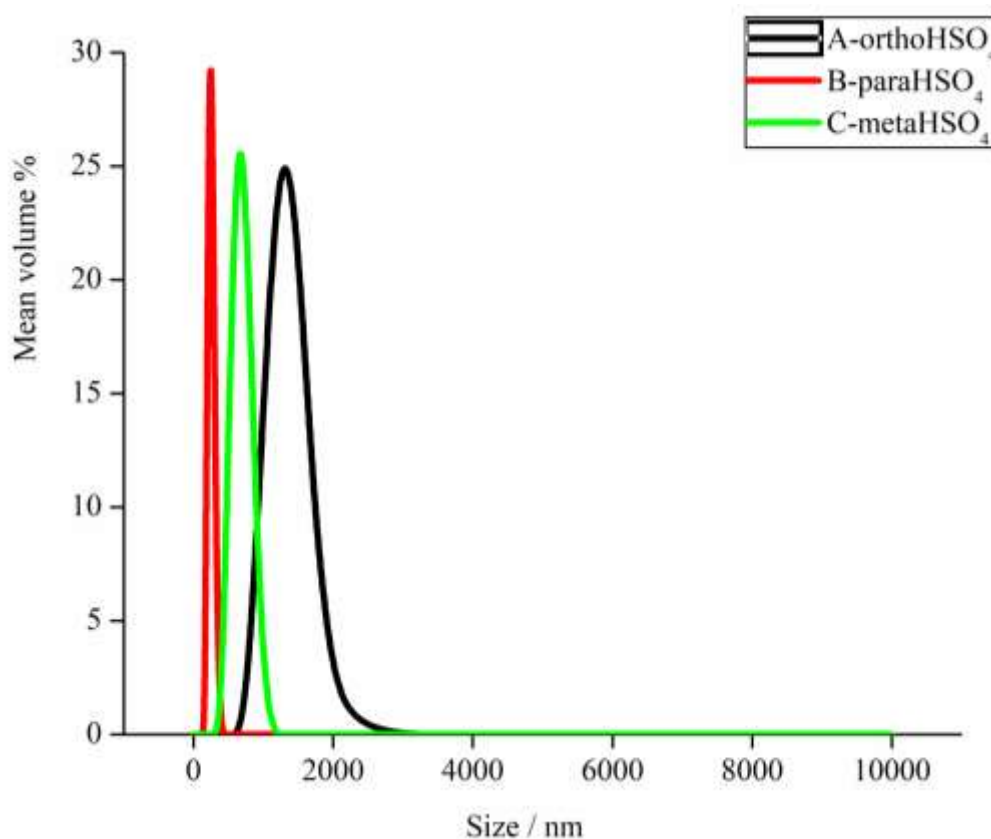
Figure 4.13: Size distribution of HSO_4 based ILs.

The order of the ILs distribution size from the biggest to the smallest are listed as below and the value are tabulated in **Table 4.8**.

B-paraCl> C-metaCl> A-orthoCl> A-orthoHSO$_4$> C-metaHSO$_4$> B-paraHSO$_4$

Table 4. 8: Diameter size of six ILs.

No.	Ionic liquids	Diameter size, nm
1	A-orthoCl	888.16
2	B-paraCl	3842.45
3	C-metaCl	3083.94
4	A-orthoHSO$_4$	1295.92
5	B-paraHSO$_4$	230.30
6	C-metaHSO$_4$	659.93

The results are in good agreement with the difference strength in binding or cohesive energy between the cation and anion (Cao et al., 2016). Indeed, it gives a clear picture on the intramolecular bonding and hydrogen bonding network were much stronger in HSO_4^- compared to Cl^- based ILs resulting in small diameter size. Besides, it illustrated the atoms and ions are bind together in form of crystal structure. Diameter size also reflects the

amount of energy needed in order to separate an atomic nucleus completely into its constituent proton and neutron. The result is consistent with reports by previous researchers as they observed through the frequency of ATR-IR and was verified through theoretical calculation (Gao et al., 2010; Jeon et al., 2008).

4.1.7 Acidity properties of all six ILs

The acid property was measured using Hammet acidity function (H_o). The value of H_o was calculated based on intrinsic pK_a of the indicator (p-nitroaniline) in water and the molar ratio of protonated and unprotonated p-nitroaniline $[I]/[IH^+]$ using Equation 4.1. The method is similar to the one used in a previous work (Chiappe et al., 2013). A low value of H_o indicates the strong ability of ILs to transfer H^+ to the base indicator.

$$H_o= pK(I)a + log \ ([I]/[IH^+]) \qquad\qquad (Eq \ 4.1)$$

Noticeable changes in the absorption of curve of p-nitroaniline in the wavelength region of 350 to 400 nm upon the addition of ILs was observed and shown in **Figure 4.14**. ILs with strong acidic anion such as HSO_4^- protonate the p-nitroaniline to a higher extent to give a lower value of H_o compared to Cl^- based ILs.
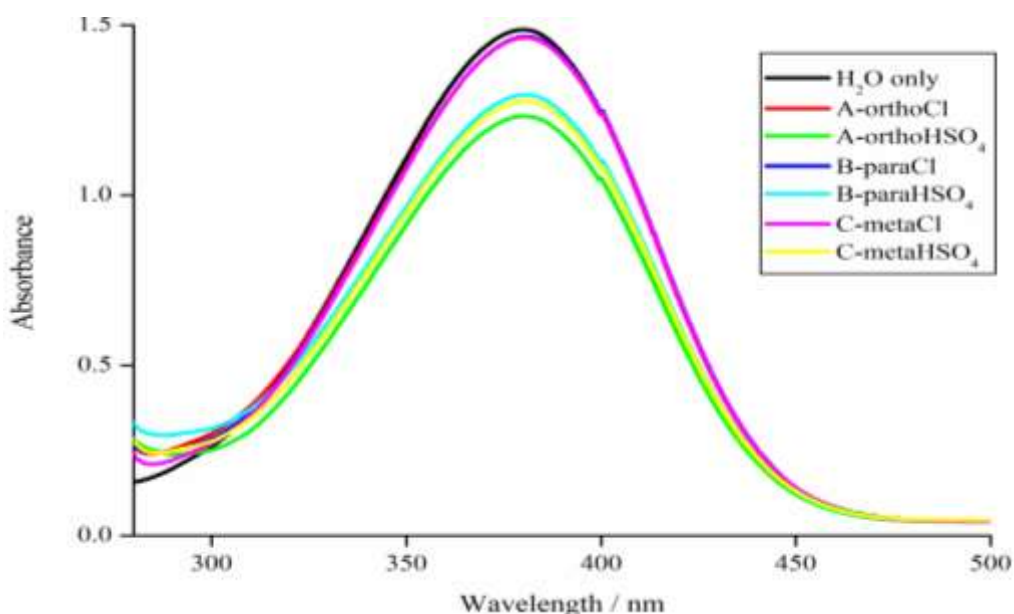
Figure 4.14: Absorbance of protonated p-nitroaniline in the absence and presence of ILs.

The data also reveals that the position of cationic sites have a small influence on acid property even though it was not significant. Interestingly, this insignificant value have lead to the understanding of the polarity difference that exist in A-ortho, B-para and C-meta as it gives an effect in the acid property of ILs. It was clearly illustrated that A-ortho is more polar than B-para and C-meta based on their H_o values. The fact that the pattern of cationic arrangement is the same for both anion species verifies this observation.

Therefore, the order of H_o values from highest to the lowest is B-paraCl> C-metaCl> A-orthoCl> B-paraHSO$_4$> C-metaHSO$_4$> A-orthoHSO$_4$.

The results in **Table 4.9** indicate the acidity of A-orthoHSO$_4$ is the strongest among these ILs. The results from this analysis become the major contribution in understanding the catalytic activity and will discuss thoroughly in **Section 4.2.**

Table 4.9: H_o value of six ILs.

Ionic liquids	Absorbance	[I] [%]	[HI] [%]	H_o
p-nitroaniline	1.486	100	0	-
A-orthoCl	1.462	98.45	1.54	2.77
B-paraCl	1.466	98.38	1.61	2.85
C-metaCl	1.464	98.65	1.34	2.79
A-orthoHSO$_4$	1.232	82.91	17.08	1.67
B-paraHSO$_4$	1.295	87.08	12.91	1.81
C-metaHSO$_4$	1.276	85.81	14.18	1.77

4.1.8 Solubility test

All six ILs possess good solubility in polar solvents mainly water, MeOH, and DMSO (**Table 4.10**). The ILs were classified as hydrophilic groups of ILs. In addition, hydrophobicity and hydrophilicity of compound are depending strongly on the anion species and can be tailor made during the synthesis process (Fukaya & Ohno, 2013; Huddleston et al., 2001; Zhang et al., 2011). Therefore, in this case Cl and HSO$_4$ anion

are expected to give good feature of hydrophilicity in the ILs system. The idea of solubility gives important and useful information for future application of dehydration of fructose.

Table 4.10: Solubility of six ILs in common solvent.

Ionic liquids	water	MeOH	DMSO	DMF	Hexane	Et$_2$O	EtOAc
A-orthoCl	M	M	M	M	I	I	I
B-paraCl	M	M	M	M	I	I	I
C-metaCl	M	M	M	M	I	I	I
A-orthoHSO$_4$	M	M	M	M	I	I	I
B-paraHSO$_4$	M	M	M	M	I	I	I
C-meaHSO$_4$	M	M	M	M	I	I	I

M =Miscible , I =Immiscible

*Measurement was conducted at room temperature (28.0 °C)

4.2 Dehydration of fructose to 5-HMF

4.2.1 Solvent effect

Three different solvents were employed in the dehydration of D-fructose to HMF for 30 min at 80 °C. The amount of the solvent used was 10 mL. The selection of the solvent were based on the previous report as it give valuable impact in the HMF production and also, the ability to set as a medium to produce a homogeneous solution (Tong & Li, 2010).

Therefore, three selected solvents were screened by using the high acidity ILs which is A-orthoHSO$_4$ (based on Hammett value, H$_o$) to acts as catalyst. The performances of the solvent were lead by DMSO as it yield 1.82 % follow by DMF and H$_2$O with 1.03 % and 0.76 % respectively. The objective of this investigation is to optimize the performance of the solvent and further use to restrict the formation of the side products by shifting the equilibrium in reaction system and suppressed the HMF hydrolysis (Ma et al., 2014;

Tong & Li, 2010). Based on the experimental data that set out in **Figure 4.15**, DMSO has been selected to use as a medium for others optimization condition of reaction temperature, reaction time and recyclability.
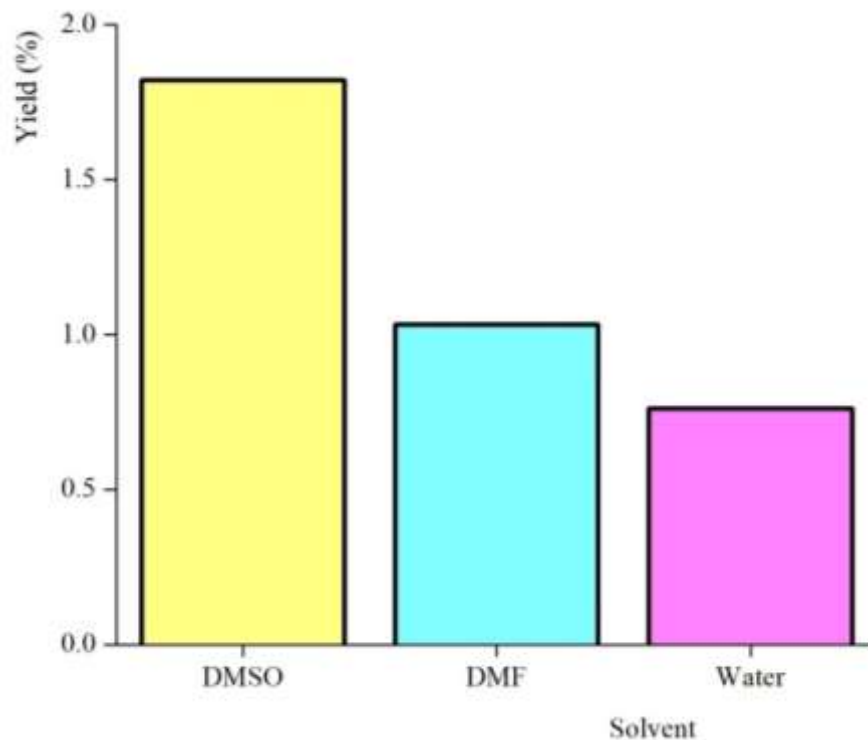
Figure 4.15: Effect of solvent on HMF yield. Reaction of fructose was performed on a 0.50 g scale of fructose at three difference solvents in the presence of 0.05 g A-orthoHSO$_4$, reaction time 30 min at temperature 80 °C.

The low yield that produced from H$_2$O can be simply understood from its low boiling point in comparison with DMSO and DMF. It eventually caused evaporation to happen thus affect the homogeneity in the reaction medium. Moreover, reaction in H$_2$O system will promote rehydration process and formation of undesirable side products of levulinic and formic acids (De et al., 2011).

Conversely, DMSO is favorable over DMF can be justify through the different relative polarity of 0.444 and 0.386, respectively (Reichardt, 2006; Sener, 2008). Hence, in this case, solvent that has high polarity and boiling point was suggested to have good solubility and give optimum interaction with fructose and catalyst. In a meantime, the

toxicity potential in DMF should be taken into account before proceed to the next level (Clayton et al., 1963; Mraz et al., 1993; Tanaka, 1971) and DMSO that consider much safer was recommended for future study. This result becomes one of the important points to understand the mechanism study of dehydration reaction of fructose using these new ILs as catalysts.

4.2.2 Six ILs as catalyst in dehydration process

To study the catalytic activity of the synthesized ILs, 0.20 g ILs is used in the dehydration of fructose in DMSO at 100°C for 60 min. The process is illustrated in **Scheme 4.1.** The ILs were dried under vacuum for 2 hours prior to reduce moisture effect. During the reaction, the color of the reaction mixture was initially pale yellow but gradually turned deep brown as the temperature and reaction time are increased. This observation indicates the formation of side products such as humins (Kotadia & Soni, 2013; Tsilomelekis et al., 2016; Zandvoort et al., 2013).
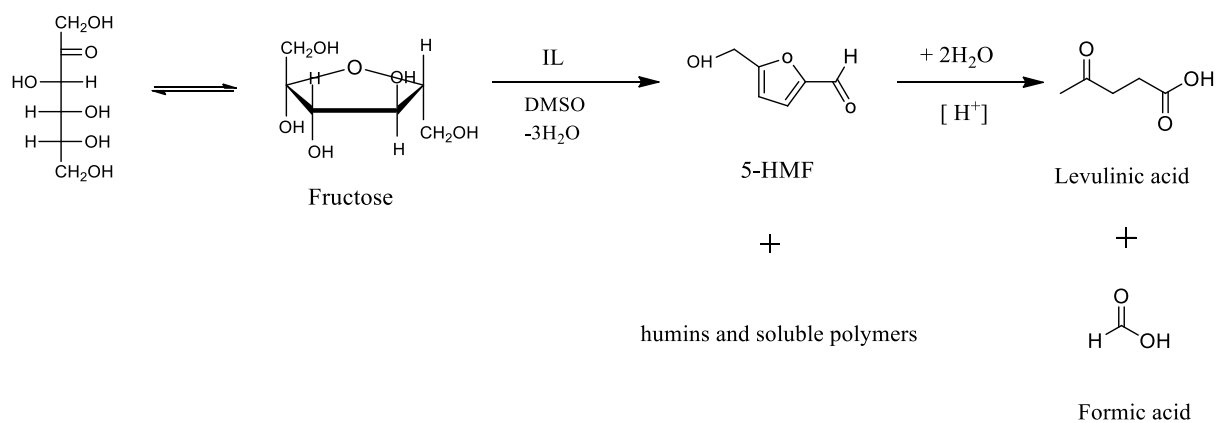
Scheme 4.1: Reaction process for dehydration of fructose.

The result as provided in **Figure 4.16** showed that A-orthoCl managed a fructose conversion of 82.8 % and HMF yield of 49.3%. On the other hand, the fructose conversion percentage and HMF yield when using C-metaCl was slightly lower, being 79.5 % and 47.0 % respectively. The usage of B-paraCl only achieved 77.1% fructose conversion and 34.3 % HMF yield under similar conditions.

A similar trend was observed when ILs with HSO_4^- was used. A-orthoHSO$_4$ was the most promising with a 95.7 % fructose conversion rate and 90.6 % of HMF yield. In the presence of C-metaHSO$_4$ and B-paraHSO$_4$, fructose conversion was 95.3 % and 93.0 % while the HMF yield was 89.1 % and 62.0 %, respectively.

The percentage of selectivity was calculated based on the fructose conversion and HMF yield. A-orthoHSO$_4$ recorded the highest selectivity, 95.0 % while C-metaHSO$_4$ and B-paraHSO$_4$ recorded 93.0 % and 66.7 % respectively. Cl$^-$ based ILs only offered lower selectivity with B-paraCl having 44.4 %, C-metaCl, 59.0 % and for A-orthoCl, 60.0 %.
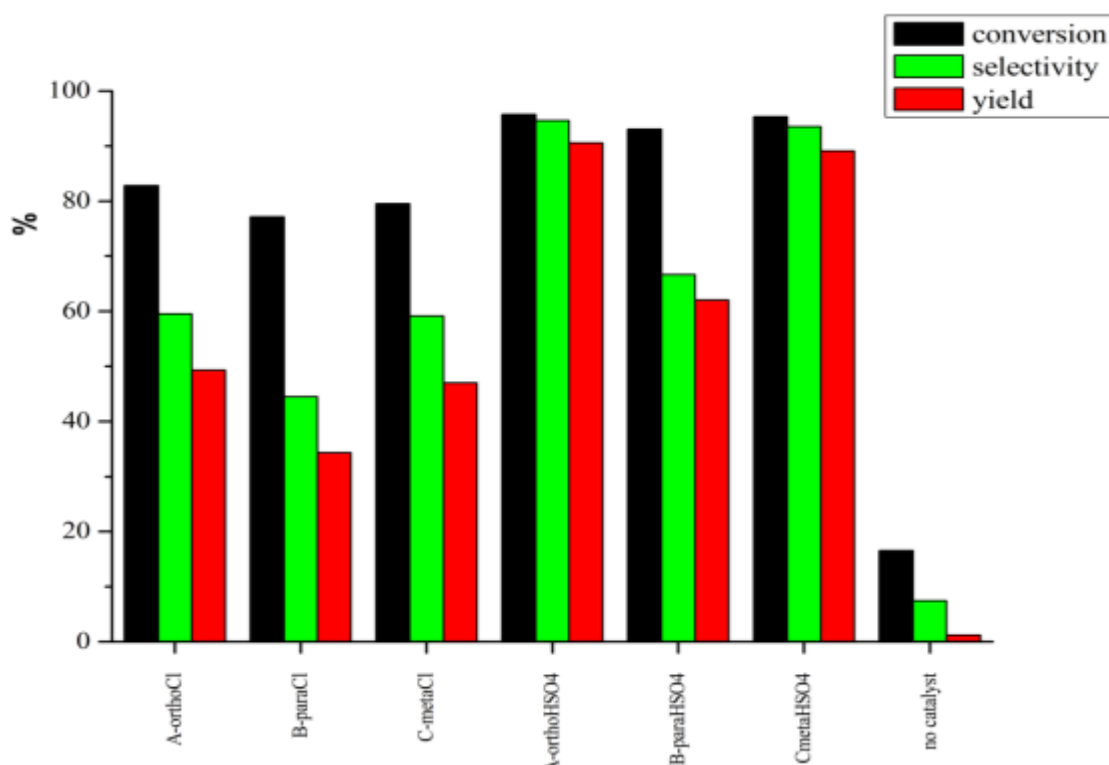
Figure 4.16: Dehydration of fructose in the presence of six ILs as catalyst. Reaction conditions (1.00 g fructose, 0.20 g ILs, 10 mL DMSO, 100 °C, 60 min).

The present study was also designed to determine the effect of anion in the preparation of HMF. What is striking about the data is that the HSO$_4$ based anion performed outstandingly with a fructose conversion of up to 95.7 % and HMF yield of up to 90.6 %. These results further support the importance of anion acidity in catalytic activity and this

correlation can be predicted with the Hammett acidity function (Bao et al., 2008; Shi et al., 2012).

The catalytic performances of ortho, meta and para cationic ILs can be rationalized by considering their difference in dipole moment and polarity. **Figure 4.17** illustrates the net resultant dipole moment (μ).
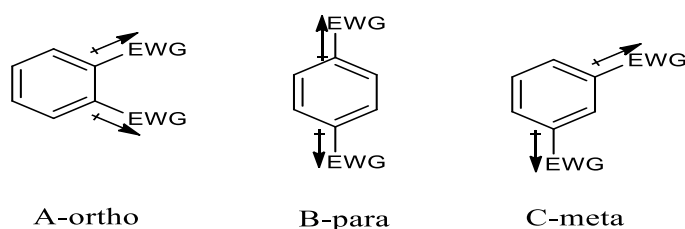
Figure 4.17: Different dipole moment in ortho, meta and para.
*EWG: Electro withdrawing group.

It can also be explained by considering,

$$\mu_{ortho} = \sqrt{\mu^2_1 + \mu^2_2 + 2\mu_1\mu_2 cos 60°}$$
$$= \sqrt{\mu^2_1 + \mu^2_2 + \mu_1\mu_2} \qquad \text{(Eq. 4.2)}$$

$$\mu_{meta} = \sqrt{\mu^2_1 + \mu^2_2 + 2\mu_1\mu_2 cos 120°}$$
$$= \sqrt{\mu^2_1 + \mu^2_2 - \mu_1\mu_2} \qquad \text{(Eq. 4.3)}$$

$$\mu_{para} = \sqrt{\mu^2_1 + \mu^2_2 + 2\mu_1\mu_2 cos 180°}$$
$$= \sqrt{\mu^2_1 + \mu^2_2 - 2\mu_1\mu_2} \qquad \text{(Eq. 4.4)}$$

From equations **(4.2)**, **(4.3)** and **(4.4)**, when both substituents are electron withdrawing, the ortho position gives the highest dipole moment whereas para gives the least. In general the trend of dipole moment is **ortho>meta>para** (Ganguly,2012; Housecroft & Sharpe, 2008). Therefore, the polarity in cationic site is important as it reflects the acidity of the C2 proton in imidazolium (**Figure 4.18**). In fact, in these dicationic ILs, the delocalization system is more effective because of the support from the three benzene rings that increase the polarity of C2-H imidazolium which in turns alleviate the acidity (Kotadia & Soni, 2013; Priede et al., 2014). As a result, the acidic behavior of cationic facilitates the

solvation mechanism in the dehydration process (Chiappe et al., 2009; Chinnappan et al., 2014). Therefore, A-orthoHSO$_4$ was chosen for further optimization on reaction time, temperature, catalyst loading and recyclability.
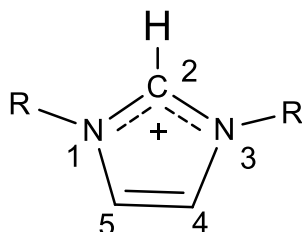
Figure 4.18: The numbering of ring atoms in imidazolium.

4.2.3 Proposed reaction mechanism

A time-progression stack of ^{1}H-NMR spectra was conducted on fructose dehydration. This experiment was carried out to further investigate the selectivity of A-orthoHSO$_4$ for HMF formation. Previous research has suggested the formation of HMF was initiated via a cyclic mechanism (De et al., 2011). The proton generated during hydrolysis assisted the reaction followed by a nucleophilic attack to obtain the final product. On the other hand, according to a mechanism proposed by Kotadia and Soni (2013), the conversion of fructose to HMF was activated by the cation that acts as an electrophile. In our case, the transformation of fructose into HMF was assisted by DMSO which not only acts as a medium, but also as an electrophile (Amarasekara et al., 2008). Then three water molecules were eliminated by the HSO$_4$anion (Kotadia & Soni, 2013). The dehydration of fructose in DMSO without catalyst resulted in a fructose conversion of about 16.6 % and HMF yield of 1.2 % which supported our previous justification (**Figure 4.16**).

According to **Figure 4.19**, as the reaction time is increased from 5 to 60 min at 100 °C, the peaks characteristic of HMF (4.45 (s), 6.55 (d), 7.45 (d), and 9.51(s) ppm) gradually increased while the fructose peaks (between 3.0 to 4.6 ppm) started to disappear. The ^{1}H-NMR recorded after 60 min reaction showed only HMF and H$_2$O (3.6

ppm) signals indicating that the fructose dehydration reaction in DMSO with A-orthoHSO$_4$ is selective for HMF formation.
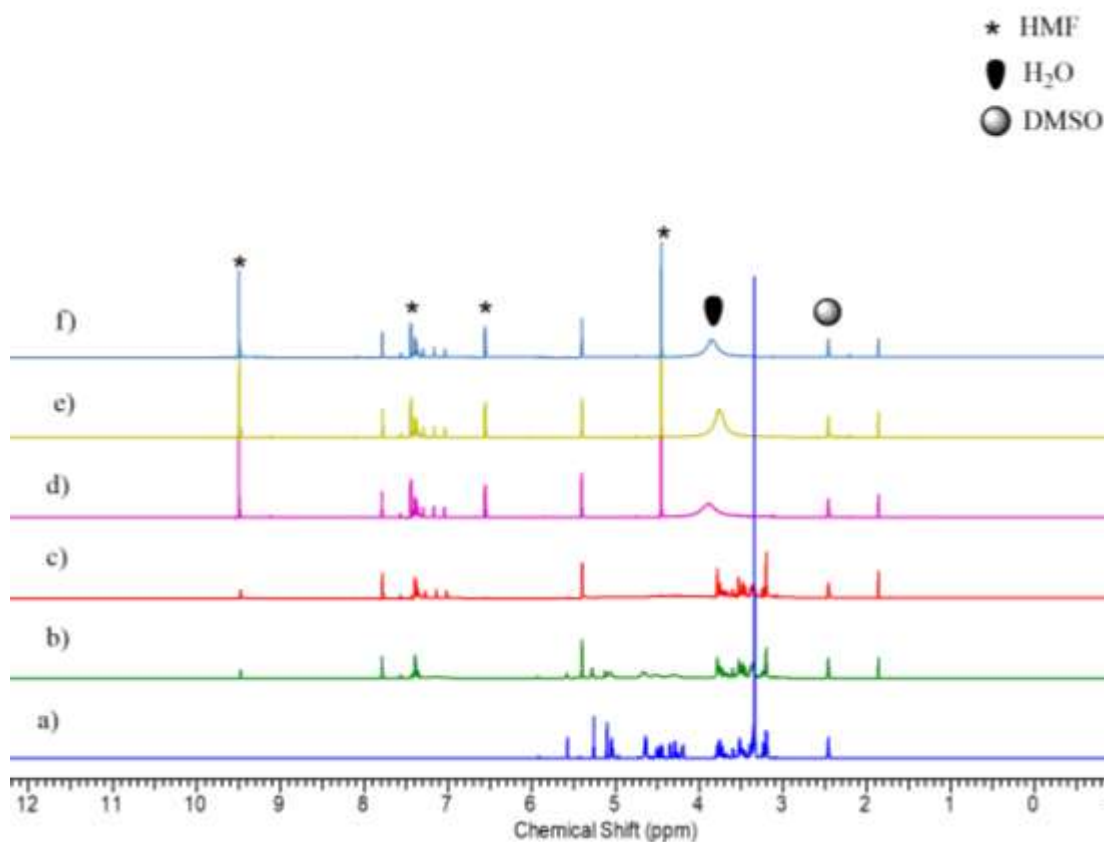
Figure 4.19: ^{1}H-NMR spectra of a) 25 mg fructose in DMSO-d$_6$ b) 25 mg fructose in DMSO-d$_6$ in the presence of 17.5 mg of A-orthoHSO$_4$ (2:1 ratio) at 0 min c) reaction at 5 min d) reaction at 20 min, e) reaction at 40 min f) reaction at 60 min.

In fact, the line broadening in our ^{1}H-NMR spectra (3 to 5ppm) presented in **Figure 4.20** indicated the hydrogen bonding between the –OH of fructose and HSO$_4^-$ is proof that this anion was responsible for eliminating the water molecules in the reaction and at the same time promoting fructose dissolution. The result from this study is consistent with the works of Tong and Li (2010).
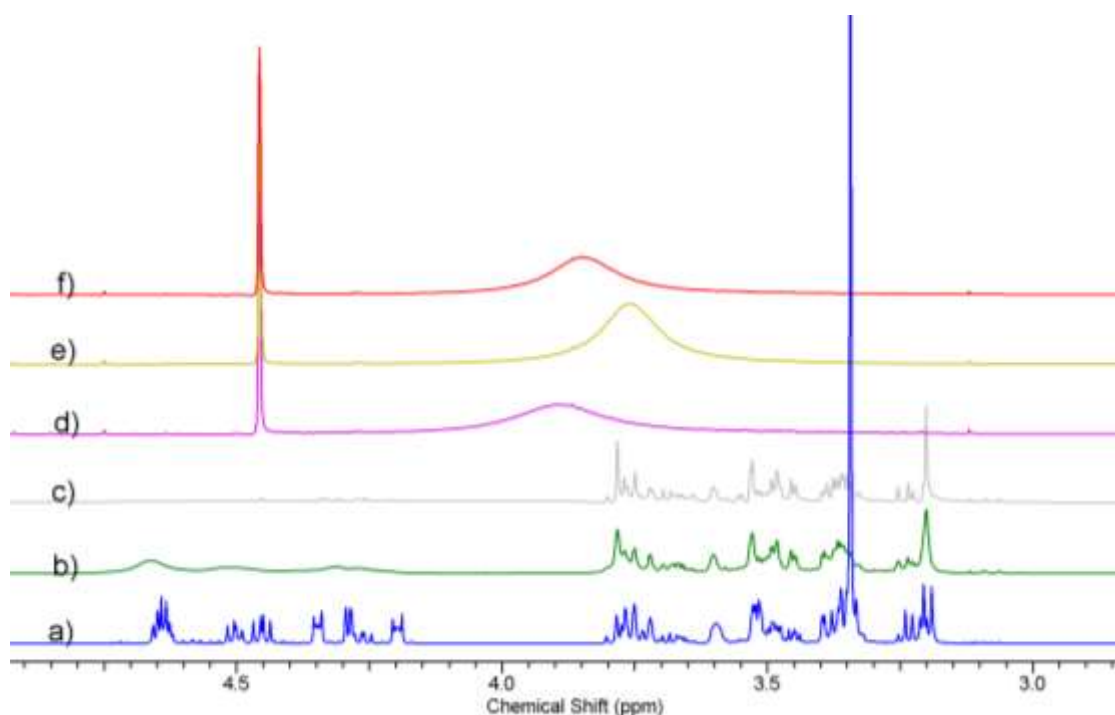
Figure 4.20: ^{1}H-NMR in the range of 3.0 to 4.5 ppm displaying the OH signal from fructose started to disappear due to the interaction with catalyst. a) 25mg fructose in DMSO-d_6 b) 25 mg fructose in DMSO-d_6 in the presence of 17.5 mg of A-orthoHSO$_4$ (2:1 ratio) at 0 min c) reaction at 5 min d) reaction at 20 min, e) reaction at 40min f) reaction at 60min.

Additionally, as illustrated in the proposed mechanism (**Scheme 4.2**), hydrogen bonding between fructose and C2-H imidazolium was assumed to accelerate the transformation process of fructose to HMF. Substantially, the specific interaction of C2-H imidazolium with oxygen atom of fructose was clearly captured in ^{1}H-NMR **(Figure 4.21)** and being demonstrated in proposed mechanism at intermediate **(3).** The interaction was recorded at min 20 of the reaction. This evidenced give a significant outcome and further highlight the important role of acidity function of C2-H imidazolium in dehydration of fructose.

Besides, this particular figure also displayed the time stacking of singlet peak of aldehyde formation at most downfield region, 9.51 ppm.
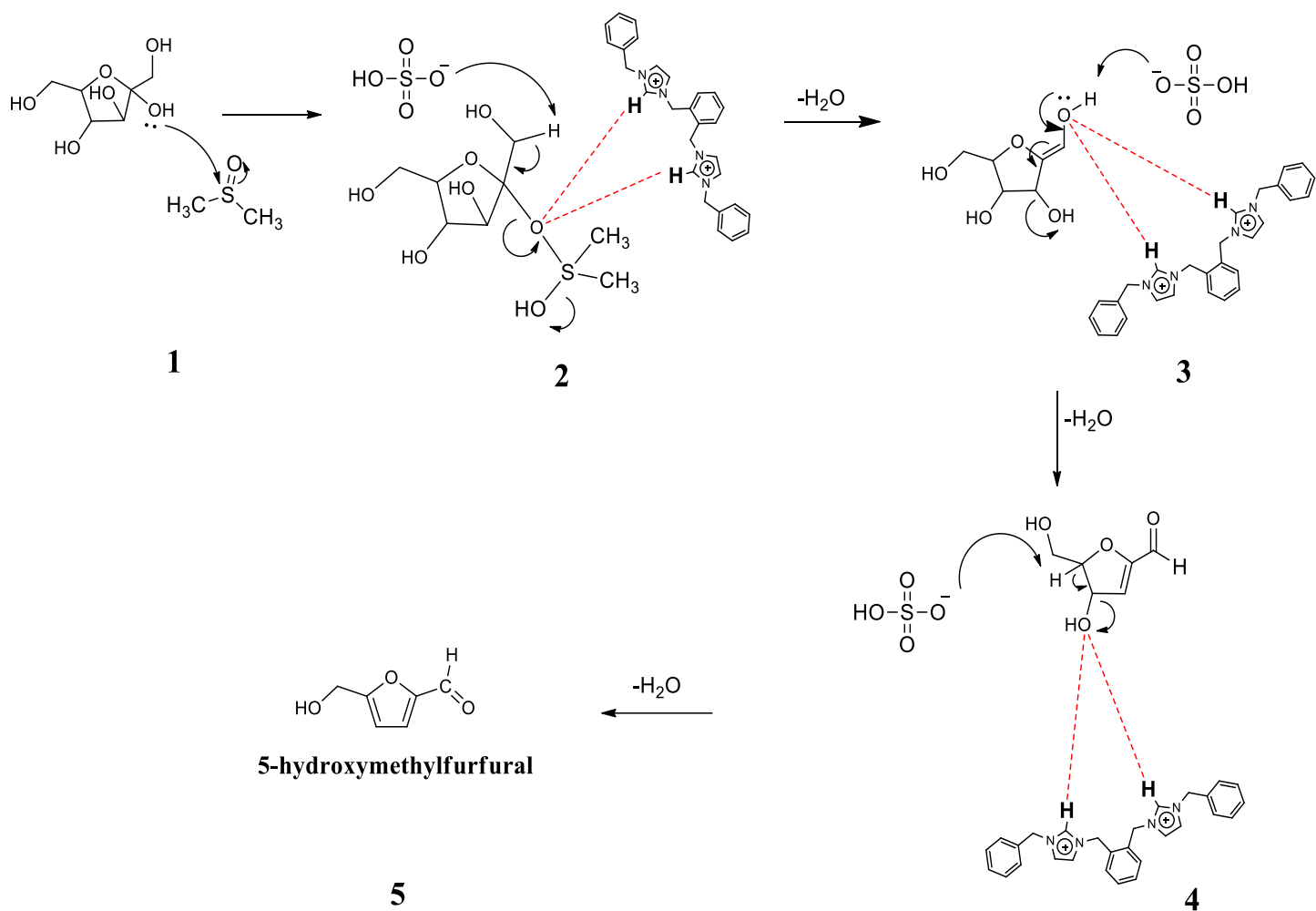
Scheme 4.2: Plausible mechanism for fructose dehydration using A-orthoHSO$_4$ catalyst. (The red dotted line represents hydrogen bonding).
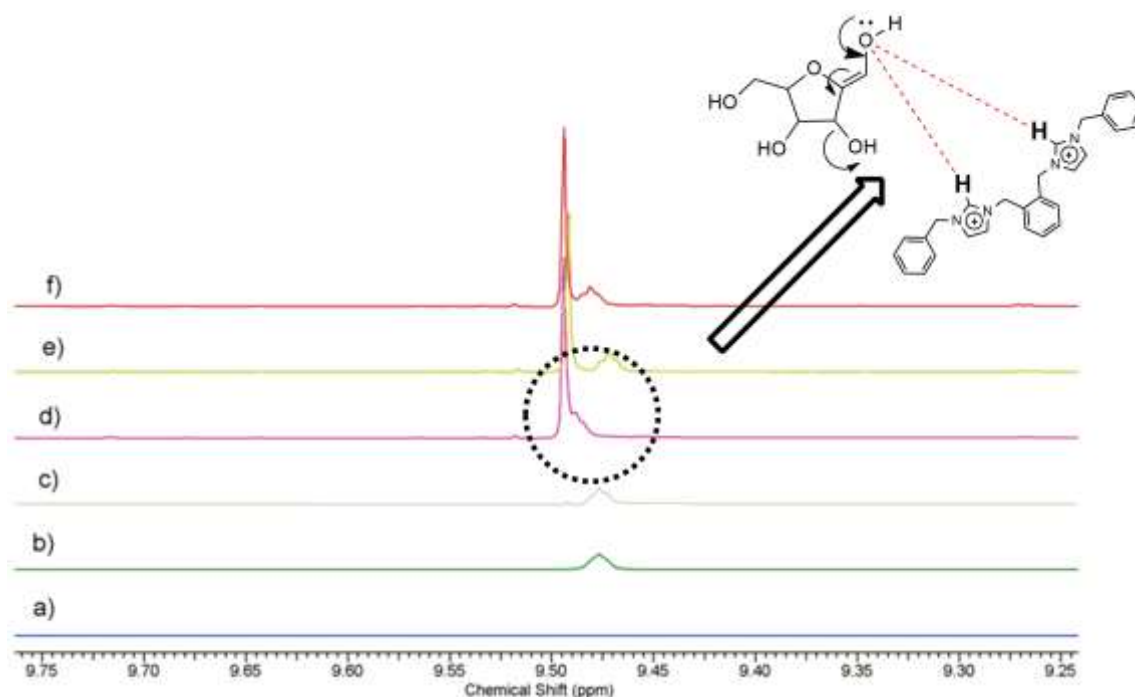
Figure 4.21:^{1}H-NMR illustrates the interaction between C2-H imidazolium and oxygen atom of fructose; a) 25 mg fructose in DMSO-d_6 b) 25 mg fructose in DMSO-d_6 in the presence of 17.5 mg of A-orthoHSO$_4$ (2:1 ratio) at 0 min c) reaction at 5 min d) reaction at 20 min, e) reaction at 40 min f) reaction at 60 min.

4.2.4 Effect of reaction temperature

The dehydration reaction of fructose was studied at 40-160 °C in order to determine the effect of reaction temperature on the formation of HMF. As explained in **Figure 4.22**, the reaction temperature plays an important role in both fructose conversion and HMF yield. When the reaction temperature was 40 °C, the conversion and yield were relatively low being only 56.4 % and 32.0 % respectively. A gradual increase in temperature to 130 °C resulted in a 98.3 % conversion and 95.1 % yield. At 160 °C, the fructose conversion increases slightly but a decrease in the HMF yield was observed. The solution color changed from light yellow to deep brown indicating the formation of side products other than HMF. This result highlighted the best reaction temperature occurred at 130 °C.
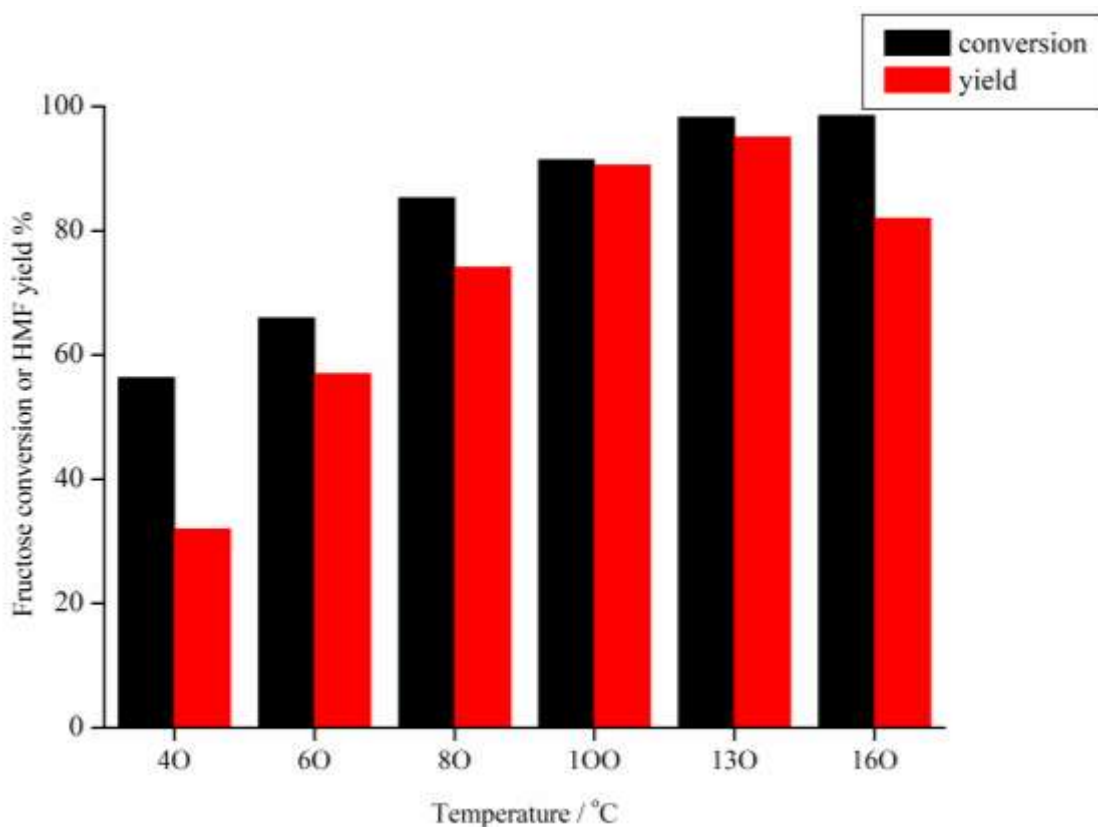
Figure 4.22: Effect of temperature on HMF yield and conversion. Reactionswere performed on a 1.00 g scale of fructose (5.5 mmol) at six reaction temperatures in the presence of 0.20 g A-orthoHSO$_4$ in DMSO (10 mL), reaction time 60 min.

4.2.5 Effect of reaction time

The dehydration time of fructose was varied to study the rate of HMF formation as a function of time. As plotted in **Figure 4.23**, the yield of HMF improved from 73.2 % to 90.5 % upon increasing the duration of reaction from 30 to 60 min at 100 °C. Further increase in the reaction time to 120 min resulted in the maximum HMF yield of 94.2 % and fructose conversion of 98.3 %. At 180 min, the production of HMF dropped to 79.9 %. These results provide an indication that, longer reaction time caused perturbation in HMF stability thus proceed to rehydration process and favor the conversion of HMF to by products (Chinnappan et al., 2014; Jadhav et al., 2014; Jadhav et al., 2012). Therefore, the optimum reaction temperature was achieved in 120 min.
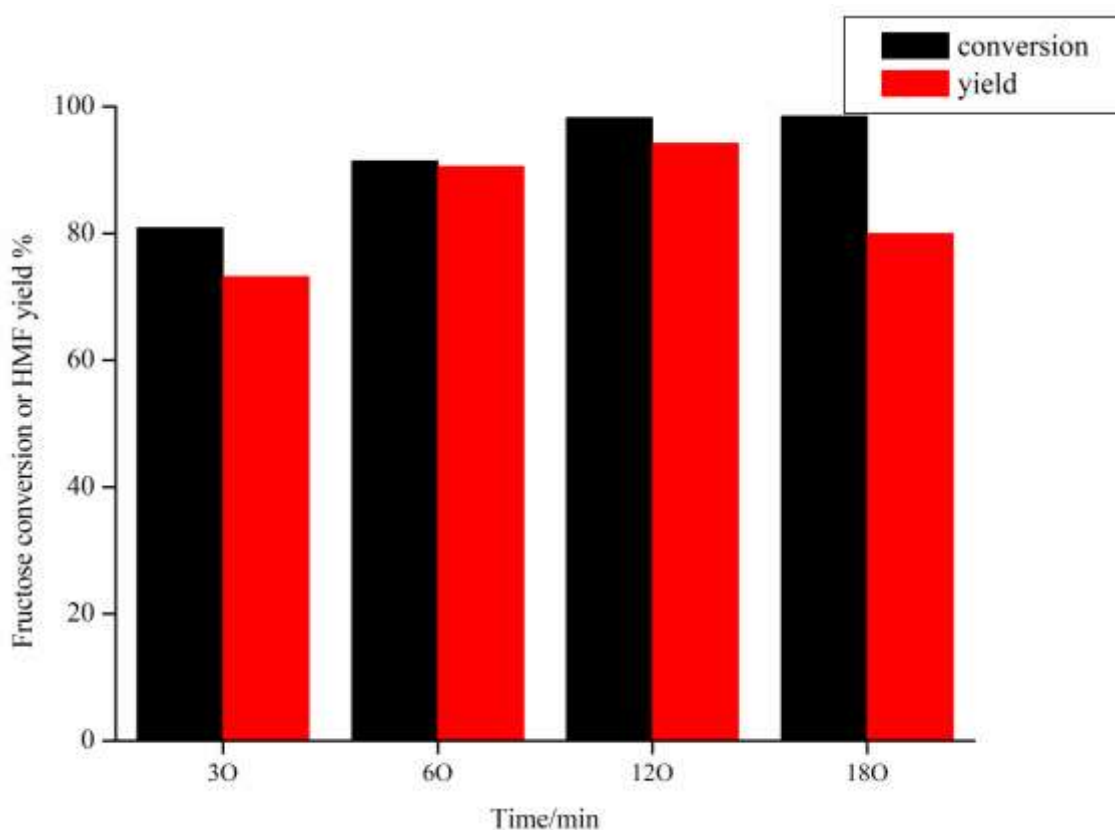
Figure 4.23: Effect of time on HMF yield and fructose conversion. Reactions were performed on a 1.00 g scale of fructose (5.5 mmol) at four different reaction time in the presence of 0.20 g A-orthoHSO$_4$ in DMSO (10 mL), temperature at 100 °C.

4.2.6 Catalyst dosage

The dehydration reaction of fructose into HMF was studied with varying dosage of A-orthoHSO$_4$ catalyst (0.01 - 1.00 g) to optimize reaction conditions and maximize HMF yield.

As shown in **Figure 4.24,** the yield of HMF increased from 32.9 % to 90.6 % with an increase in catalyst from 0.01 to 0.20 g. When the amount of catalyst is further increased, the yield of HMF decrease to 24.5 % and the fructose conversion becomes 98.7 %.It also noted that the brown solution turned darker when 1.00 g catalyst is used. As Illustrated in **scheme 4.1** previously, it was predicted that besides humins, levulinic acid and formic acid are also formed (Jadhav et al., 2014; Jadhav et al., 2013). The side products are confirmed by ^{1}H-NMR to exist whenever three samples from the maximum temperature

(160 °C), reaction time (180 min), and catalyst dosage (1.00 g) are used respectively.

Figure 4.25 display two different regions; the downfield region (δ 8.09 ppm) indicating –COOH resonance of formic acid, and the upfield region (δ 2.32 ppm, 2.65 ppm and 2.67 ppm) being the fingerprint of levulinic acid (De et al., 2011; J. Zhang & Weitz, 2012). It is interesting to note that a possible explanation for the formation of side products is the presence of excess acidic sites and water allowed rehydration to occur (Kotadia & Soni, 2013).
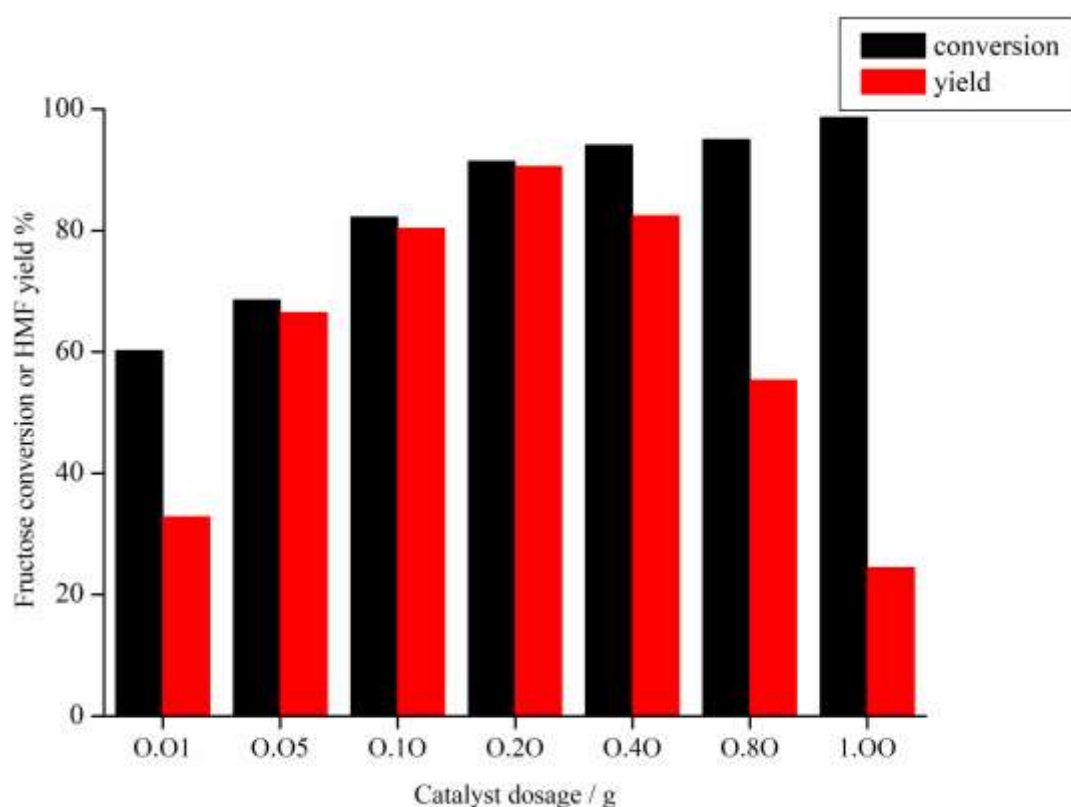
Figure 4.24: Effect of catalyst loading on HMF yield and fructose conversion. Reactions were performed on a 1.00 g scale of fructose (5.5 mmol) at seven different catalyst dosages in DMSO (10 mL), reaction time 60min and temperature at 100°C.
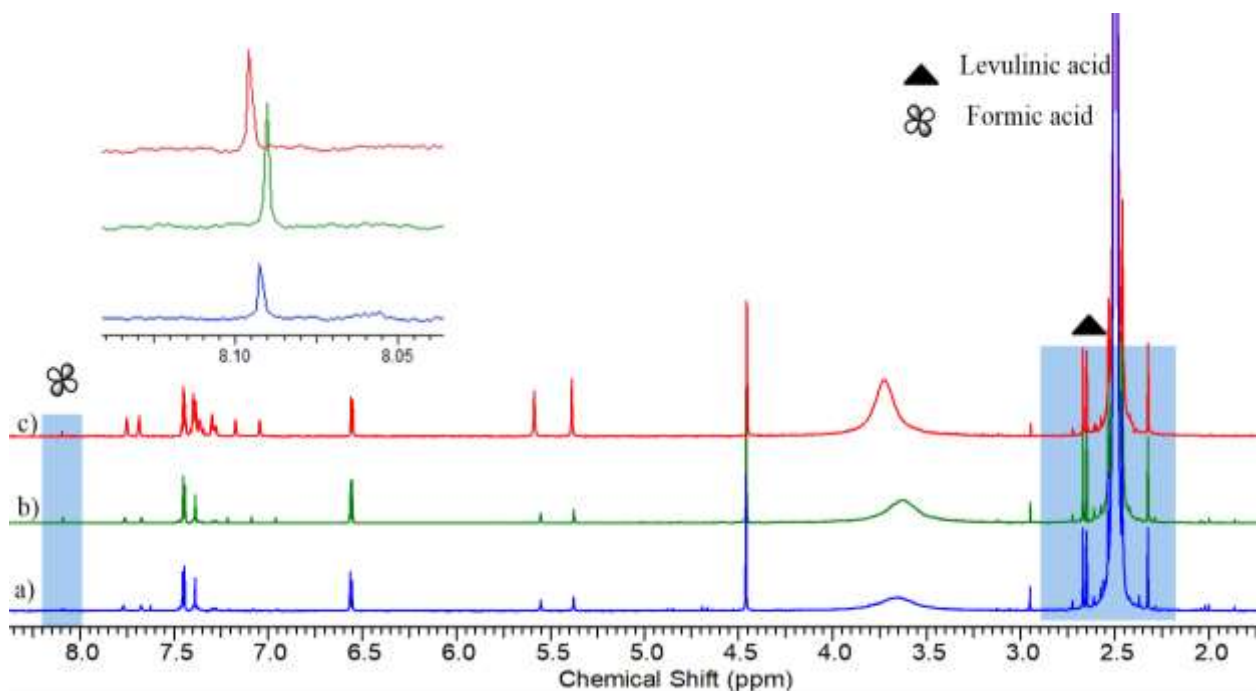
Figure 4.25: A representative ^{1}H-NMR (DMSO- D_6) spectrum of the reaction product obtained from the dehydration reaction of the reaction a) highest temperature (160 °C) b) longest reaction time (180 min) c) maximum catalyst loading (1.00 g).

4.2.7 The recycling of catalyst and solvent

The feasibility in recycling A-orthoHSO$_4$ and DMSO were examined. Prior to each cycle, the ILs and DMSO were extracted using ethyl acetate. The HMF mostly moved to the organic phase leaving a negligible trace in the aqueous phase (Tsilomelekis et al., 2014) while the ILs and DMSO remained in the aqueous phase. **Figure 4.26** show that the loss of activity is in the range of 2.7 to 9.5 % per cycle. In comparison with the study from Jadhav et al (2012) stated that, no outstanding loss during the recyclable study as the conversion achieved 100 % with yield 82 % over six cycles. Loss of yield is attributed to the loss of ILs during the extraction step that reduced effectiveness in reaction.
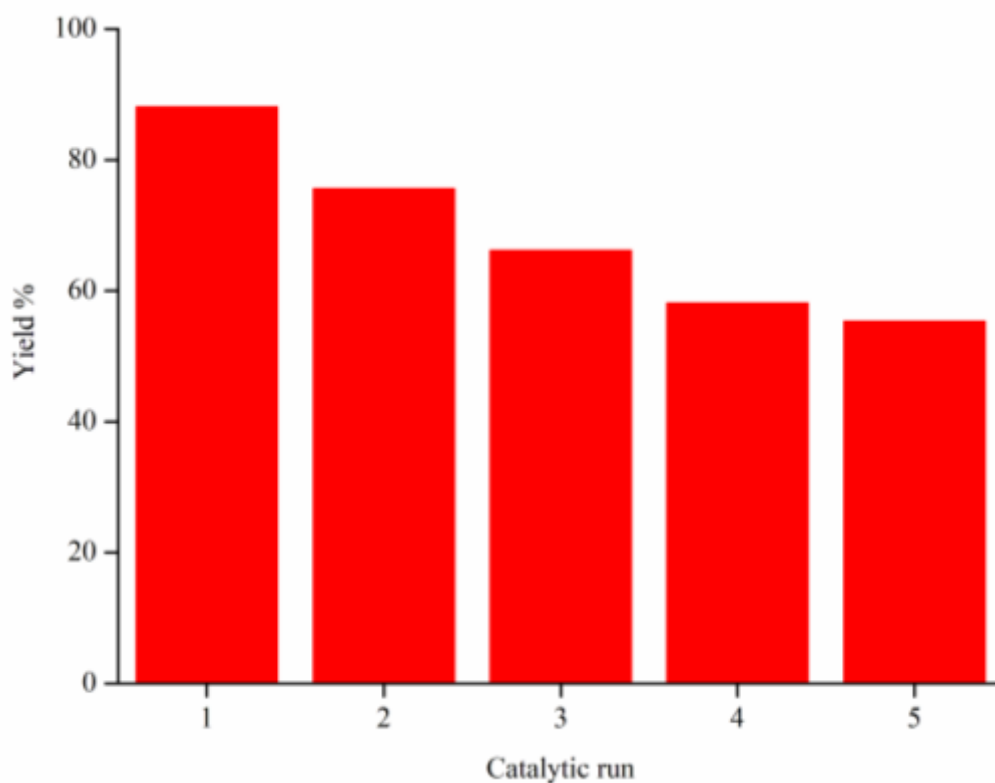
Figure 4.26: Recyclability of A-orthoHSO$_4$ and DMSO for dehydration reaction. Reaction condition for each run: fructose (1 g, 5.5 mmol), 0.20 g A-orthoHSO$_4$ (recycled), reaction time: 60 min, temperature: 100 °C.

The capability and effectiveness of our catalysts in dehydration reaction is tabulated in **Table 4.11**. This table also provided a possible adjustment parameter from different synthesized ILs. The outcome can be seen from the percentage yield of HMF with different temperature range and reaction time used. Besides, the role of DMSO in dehydration reaction can be justified.

Table 4.11: Different ILs used in dehydration process.

No	Catalysed used	Solvent	T/ °C	t/ min	HMF yield %	Reference
1	[DiEG(mim)$_2$][OMs]$_2$	-	120	40	69.8	(Jadhav et al., 2012)
2	[TriEG(mim)$_2$][OMs]$_2$	-	120	40	77.2	(Jadhav et al., 2012)
3	[TetraEG(mim)$_2$][OMs]$_2$	-	120	40	92.3	(Jadhav et al., 2012)
4	[C$_6$(mpy)$_2$]$_2$Br	DMSO	110	60	91.0	(Chinnappan et al., 2014)
5	[C$_{10}$(Epy)$_2$]$_2$Br	DMSO	110	60	83.0	(Chinnappan et al., 2014)
6	[NMP]$^+$[HSO$_4$]$^-$	DMSO	90	120	69.4	(Tong & Li, 2010)
7	[Mim][HSO$_4$]	DMSO	90	120	23.6	(Tong & Li, 2010)
8	[NMP]$^+$[CH$_3$SO$_3$]$^-$	DMSO	90	120	72.3	(Tong & Li, 2010)
9	[PSMBIM]HSO$_4$	DMSO	80	60	72.8	(Kotadia & Soni, 2013)
10	A-orthoHSO$_4$	DMSO	100	60	90.5	This work
11	B-paraHSO$_4$	DMSO	100	60	62.0	This work
12	C-metaHSO$_4$	DMSO	100	60	89.1	This work

CHAPTER 5: CONCLUSION

5.1 Conclusion

In conclusion, six new dicationic ILs; A-orthoCl, B-paraCl, C-metaCl, A-orthoHSO$_4$, B-paraHSO$_4$, and C-metaHSO$_4$ have been successfully synthesized and characterized. The findings from this investigation complement earlier studies regarding the role of ILs and DMSO in dehydration of fructose. The use of ILs improved the percentage yield of HMF from 1.2 % (without ILs) to >30.0 % (with ILs). Besides, new reaction mechanism has been proposed with promising evidence from ^{1}H-NMR as it was clearly illustrated important role of DMSO and ILs.

The present study has confirmed the previous findings and contributed additional evidence that suggests the importance of acidic behavior of the anion in the dehydration of fructose. Furthermore, this work revealed the relative position of the substituent (ortho, meta, and para) impact the cationic C2-H imidazolium polarity which affects catalytic activity and HMF production. This finding has important implication for developing new catalyst as it gives a clear understanding regarding the distinct of chemical and physical properties of this isomer. Among the synthesized ILs, A-orthoHSO$_4$ showed high catalytic activity with a fructose conversion rate of 95.7 % and HMF yield of 90.5 % after 60 min at 100 °C after being optimized for reaction time, reaction temperature, and catalyst loading. In fact, two side products, formic acid and levulinic acid are identified using ^{1}H-NMR qualitative analysis in this dehydration process.

The investigation regarding catalyst properties and reaction parameters condition are vital for improving the biomass industry in the future. All in all, the conclusion of this study indicates that all the objectives successfully achieved and a concrete framework research analysis for future endeavors is provided.

5.2 Recommendations for future research

1. Expand the research to pyridium or pyrrolidium based ILs as comparison with the present work.

2. This work can be expanded by using readily abundant weed plants that rich with polymeric carbohydrate as a substrates for production of HMF. This approach is very useful to study the ILs performance as catalyst and outline the mechanism aspect thoroughly.

3. Adequate investigation is required to improve the recyclability of ILs. A combination of polymeric material with ILs can help to regenerate the catalyst efficiently without any apparent loses in order to sustain the high yield of product in every cycle.

4. Use microwave irradiation instead of oil bath heating for dehydration as it should reduce the reaction time effectively and at the same time be more cost effective.

REFERENCES

Amarasekara, A. S., Williams, L. D., & Ebede, C. C. (2008). Mechanism of the dehydration of d-fructose to 5-hydroxymethylfurfural in dimethyl sulfoxide at 150 °C: an NMR study. *Carbohydrate Research, 343*(18), 3021-3024.

Anderson, J. L., Ding, J., Welton, T., & Armstrong, D. W. (2002). Characterizing ionic liquids on the basis of multiple solvation interactions. *Journal of the American Chemical Society, 124*(47), 14247-14254.

Anwar, Z., Gulfraz, M., & Irshad, M. (2014). Agro-industrial lignocellulosic biomass a key to unlock the future bio-energy: a brief review. *Journal of Radiation Research and Applied Sciences, 7*(2), 163-173.

Bajpai, P. (2016). *Pretreatment of lignocellulosic biomass for biofuel production*: Springer.

Bao, Q., Qiao, K., Tomida, D., & Yokoyama, C. (2008). Preparation of 5-hydroymethylfurfural by dehydration of fructose in the presence of acidic ionic liquid. *Catalysis Communications, 9*(6), 1383-1388.

Cadenas, A., & Cabezudo, S. (1998). Biofuels as sustainable technologies: perspectives for less developed countries. *Technological Forecasting and Social Change, 58*(1–2), 83-103.

Cantero, D. A., Bermejo, M. D., & Cocero, M. J. (2015). Reaction engineering for process intensification of supercritical water biomass refining. *The Journal of Supercritical Fluids, 96*, 21-35.

Cao, S., Tao, F., Tang, Y., Li, Y., & Yu, J. (2016). Size and shape dependent catalytic performances of oxidation and reduction reactions on nanocatalysts. *Chemical Society Reviews, 45*(17), 4747-4765.

Chiappe, C., & Pieraccini, D. (2005). Ionic liquids: solvent properties and organic reactivity. *Journal of Physical Organic Chemistry, 18*(4), 275-297.

Chiappe, C., Malvaldi, M., & Pomelli Christian, S. (2009). Ionic liquids: solvation ability and polarity. *Pure and Applied Chemistry* ,81,.767.

Chiappe, C., Rajamani, S., & D'Andrea, F. (2013). A dramatic effect of the ionic liquid structure in esterification reactions in protic ionic media. *Green Chemistry, 15*(1), 137-143.

Chinnappan, A., & Kim, H. (2012). Environmentally benign catalyst: synthesis, characterization, and properties of pyridinium dicationic molten salts (ionic liquids) and use of application in esterification. *Chemical Engineering Journal, 187*, 283-288.

Chinnappan, A., Jadhav, A. H., Kim, H., & Chung, W.J. (2014). Ionic liquid with metal complexes: an efficient catalyst for selective dehydration of fructose to 5-hydroxymethylfurfural. *Chemical Engineering Journal, 237*, 95-100.

Choudhury, A. R., Winterton, N., Steiner, A., Cooper, A. I., & Johnson, K. A. (2005). In situ crystallization of low-melting ionic liquids. *Journal of the American Chemical Society, 127*(48), 16792-16793.

Clayton, J. W., Barnes, J. R., Hood, D. B., & Schepers, G. W. H. (1963). The inhalation toxicity of dimethylformamide (DMF). *American Industrial Hygiene Association Journal, 24*(2), 144-154.

De, S., Dutta, S., & Saha, B. (2011). Microwave assisted conversion of carbohydrates and biopolymers to 5-hydroxymethylfurfural with aluminium chloride catalyst in water. *Green Chemistry, 13*(10), 2859-2868.

De Souza, R. F., Padilha, J. C., Gonçalves, R. S., & Dupont, J. (2003). Room temperature dialkylimidazolium ionic liquid-based fuel cells. *Electrochemistry Communications, 5*(8), 728-731.

Demirbas, A. (2008). The importance of bioethanol and biodiesel from biomass. *Energy Sources, Part B, 3*(2), 177-185.

Duarte, A. R. C. (2009). *Current Trends of Supercritical Fluid Technology in Pharmaceutical, Nutraceutical and Food Processing Industries*: Bentham eBooks.

Erdmenger, T., Vitz, J., Wiesbrock, F., & Schubert, U. S. (2008). Influence of different branched alkyl side chains on the properties of imidazolium-based ionic liquids. *Journal of Materials Chemistry, 18*(43), 5267-5273.

Fredlake, C. P., Crosthwaite, J. M., Hert, D. G., Aki, S. N. V. K., & Brennecke, J. F. (2004). Thermophysical properties of imidazolium based ionic liquids. *Journal of Chemical & Engineering Data, 49*(4), 954-964.

Fukaya, Y., & Ohno, H. (2013). Hydrophobic and polar ionic liquids. *Physical Chemistry Chemical Physics, 15*(11), 4066-4072.

Fumino, K., Wulf, A., & Ludwig, R. (2008). Strong, localized, and directional hydrogen bonds fluidize ionic liquids. *Angewandte Chemie International Edition, 47*(45), 8731-8734.

Ganguly, A. (2012). *Fundamentals of Inorganic Chemistry*. India:Pearson Education.

Gao, Y., Zhang, L., Wang, Y., & Li, H. (2010). Probing electron density of H-bonding between cation−anion of imidazolium-based ionic liquids with different anions by vibrational spectroscopy. *The Journal of Physical Chemistry B, 114*(8), 2828-2833.

Ha, S. H., Menchavez, R. N., & Koo, Y.M. (2010). Reprocessing of spent nuclear waste using ionic liquids. *Korean Journal of Chemical Engineering, 27*(5), 1360-1365.

Holbrey, J. D., Turner, M. B., & Rogers, R. D. (2003). *Selection of ionic liquids for green chemical applications*: ACS Publications.

Housecroft, C. E., & Sharpe, A. G. (2008). *Inorganic Chemistry.* India: Pearson Prentice Hall.

Huddleston, J., & Rogers, R. (1998). Room temperature ionic liquids as novel media for 'clean' liquid–liquid extraction. *Chemical Communications*(16), 1765-1766.

Huddleston, J. G., Visser, A. E., Reichert, W. M., Willauer, H. D., Broker, G. A., & Rogers, R. D. (2001). Characterization and comparison of hydrophilic and hydrophobic room temperature ionic liquids incorporating the imidazolium cation. *Green Chemistry, 3*(4), 156-164.

Imhof, P., & van der Waal, J. C. (2013). *Catalytic Process Development for Renewable Materials*: Wiley.

Imteyaz Alam, M., De, S., Dutta, S., & Saha, B. (2012). Solid-acid and ionic-liquid catalyzed one-pot transformation of biorenewable substrates into a platform chemical and a promising biofuel. *RSC Advances, 2*(17), 6890-6896.

Ishida, T., & Shirota, H. (2013). Dicationic versus monocationic ionic liquids: distinctive ionic dynamics and dynamical heterogeneity. *The Journal of Physical Chemistry B, 117*(4), 1136-1150.

Jaccard, M. (2006). *Sustainable Fossil Fuels: The Unusual Suspect in the Quest for Clean and Enduring Energy*: Cambridge University Press.

Jadhav, A. H., Chinnappan, A., Patil, R. H., Kostjuk, S. V., & Kim, H. (2014). Green chemical conversion of fructose into 5-hydroxymethylfurfural (HMF) using unsymmetrical dicationic ionic liquids under mild reaction condition. *Chemical Engineering Journal, 243*, 92-98.

Jadhav, A. H., Kim, H., & Hwang, I. T. (2012). Efficient selective dehydration of fructose and sucrose into 5-hydroxymethylfurfural (HMF) using dicationic room temperature ionic liquids as a catalyst. *Catalysis Communications, 21*, 96-103.

Jadhav, A. H., Kim, H., & Hwang, I. T. (2013). An efficient and heterogeneous recyclable silicotungstic acid with modified acid sites as a catalyst for conversion of fructose and sucrose into 5-hydroxymethylfurfural in superheated water. *Bioresource Technology, 132*, 342-350.

Jae-An, C., Jin-Woo, L., Young-Byung, Y., Seong-Sig, H., & Chung-Han, C. (2010). Direct conversion of starch to hydroxymethylfurfural in the presence of an ionic liquid with metal chloride. *Starch - Stärke, 62*(6), 326-330.

James, O. O., Maity, S., Usman, L. A., Ajanaku, K. O., Ajani, O. O., Siyanbola, T. O., . . . Chaubey, R. (2010). Towards the conversion of carbohydrate biomass feedstocks to biofuels via hydroxylmethylfurfural. *Energy & Environmental Science, 3*(12), 1833-1850.

Jeon, Y., Sung, J., Seo, C., Lim, H., Cheong, H., Kang, M., . . . Kim, D. (2008). Structures of ionic liquids with different anions studied by infrared vibration spectroscopy. *The Journal of Physical Chemistry B, 112*(15), 4735-4740.

Kishi, H., Akamatsu, Y., Noguchi, M., Fujita, A., Matsuda, S., & Nishida, H. (2011). Synthesis of epoxy resins from alcohol-liquefied wood and the mechanical properties of the cured resins. *Journal of Applied Polymer Science, 120*(2), 745-751.

Kotadia, D. A., & Soni, S. S. (2013). Symmetrical and unsymmetrical Bronsted acidic ionic liquids for the effective conversion of fructose to 5-hydroxymethyl furfural. *Catalysis Science & Technology, 3*(2), 469-474.

Kruse, A., & Dahmen, N. (2015). Water a magic solvent for biomass conversion. *The Journal of Supercritical Fluids, 96*, 36-45.

Kunz, W., & Häckl, K. (2016). The hype with ionic liquids as solvents. *Chemical Physics Letters, 661*, 6-12.

Li, C., Zhao, Z. K., Wang, A., Zheng, M., & Zhang, T. (2010). Production of 5-hydroxymethylfurfural in ionic liquids under high fructose concentration conditions. *Carbohydrate Research, 345*(13), 1846-1850.

Lu, W., Fadeev, A. G., Qi, B., Smela, E., Mattes, B. R., Ding, J., . . . Wallace, G. G. (2002). Use of ionic liquids for π-conjugated polymer electrochemical devices. *Science, 297*(5583), 983-987.

Ma, C., Sun, Z., Chen, C., Zhang, L., & Zhu, S. (2014). Simultaneous separation and determination of fructose, sorbitol, glucose and sucrose in fruits by HPLC–ELSD. *Food Chemistry, 145*, 784-788.

Ma, Y., Qing, S., Wang, L., Islam, N., Guan, S., Gao, Z., . . . Wang, T. (2015). Production of 5-hydroxymethylfurfural from fructose by a thermo-regulated and recyclable Bronsted acidic ionic liquid catalyst. *RSC Advances, 5*(59), 47377-47383.

Marrucho, I., Branco, L., & Rebelo, L. (2014). Ionic liquids in pharmaceutical applications. *Annual review of chemical and biomolecular engineering, 5*, 527-546.

Matuszek, K., Chrobok, A., Coleman, F., Seddon, K. R., & Swadźba-Kwaśny, M. (2014). Tailoring ionic liquid catalysts: structure, acidity and catalytic activity of protonic ionic liquids based on anionic clusters,$[(HSO_4)(H_2SO_4) x]−(x= 0, 1, or 2)$. *Green Chemistry, 16*(7), 3463-3471.

Mondal, S. S., Müller, H., Junginger, M., Kelling, A., Schilde, U., Strehmel, V., & Holdt, H. J. (2014). Imidazolium 2-Substituted 4, 5-dicyanoimidazolate ionic liquids: synthesis, crystal structures and structure thermal property relationships. *Chemistry-A European Journal, 20*(26), 8170-8181.

Mraz, J., Jheeta, P., Gescher, A., Hyland, R., Thummel, K., & Threadgill, M. D. (1993). Investigation of the mechanistic basis of N,N-dimethylformamide toxicity. Metabolism of N,N-dimethylformamide and its deuterated isotopomers by cytochrome P450 2E1. *Chemical Research in Toxicology, 6*(2), 197-207.

Musau, R. M., & Munavu, R. M. (1987). The preparation of 5-hydroxymethyl-2-furaldehyde (HMF) from d-fructose in the presence of DMSO. *Biomass, 13*(1), 67-74.

Nakashima, K., Kubota, F., Maruyama, T., & Goto, M. (2005). Feasibility of ionic liquids as alternative separation media for industrial solvent extraction processes. *Industrial & Engineering Chemistry Research, 44*(12), 4368-4372.

Nikolla, E., Román-Leshkov, Y., Moliner, M., & Davis, M. E. (2011). "One-pot" synthesis of 5-(hydroxymethyl) furfural from carbohydrates using tin-beta zeolite. *ACS Catalysis, 1*(4), 408-410.

Noack, K., Schulz, P. S., Paape, N., Kiefer, J., Wasserscheid, P., & Leipertz, A. (2010). The role of the C2 position in interionic interactions of imidazolium based ionic liquids: a vibrational and NMR spectroscopic study. *Physical Chemistry Chemical Physics, 12*(42), 14153-14161.

Ohara, M., Takagaki, A., Nishimura, S., & Ebitani, K. (2010). Syntheses of 5-hydroxymethylfurfural and levoglucosan by selective dehydration of glucose using solid acid and base catalysts. *Applied Catalysis A: General, 383*(1), 149-155.

Pagán-Torres, Y. J., Wang, T., Gallo, J. M. R., Shanks, B. H., & Dumesic, J. A. (2012). Production of 5-hydroxymethylfurfural from glucose using a combination of Lewis and Brønsted acid catalysts in water in a biphasic reactor with an alkylphenol solvent. *ACS Catalysis, 2*(6), 930-934.

Pavia, D. L., Lampman, G. M., & Kriz, G. S. (2010). *Spectroscopy*: Brooks/Cole, Cengage Learning.

Priede, E., Nakurte, I., & Zicmanis, A. (2014). Structure effect of imidazolium-based dicationic ionic liquids on Claisen rearrangement. *Synthetic Communications, 44*(12), 1803-1809.

Qi, X., Guo, H., & Li, L. (2011). Efficient conversion of fructose to 5-hydroxymethylfurfural catalyzed by sulfated zirconia in ionic liquids. *Industrial & Engineering Chemistry Research, 50*(13), 7985-7989.

Qi, X., Watanabe, M., Aida, T. M., & Smith Jr, R. L. (2008). Catalytic dehydration of fructose into 5-hydroxymethylfurfural by ion-exchange resin in mixed-aqueous system by microwave heating. *Green Chemistry, 10*(7), 799-805.

Qi, X., Watanabe, M., Aida, T. M., & Smith, J. R. L. (2009). Efficient process for conversion of fructose to 5-hydroxymethylfurfural with ionic liquids. *Green Chemistry, 11*(9), 1327-1331.

Raja Shahrom, M. S., Wilfred, C. D., & Taha, A. K. Z. (2016). CO_2 capture by task specific ionic liquids (TSILs) and polymerized ionic liquids (PILs and AAPILs). *Journal of Molecular Liquids, 219*, 306-312.

Ratti, R. (2014). Ionic Liquids: Synthesis and Applications in Catalysis. *Advances in Chemistry, 2014*, 16.

Reichardt, C. (2006). *Solvents and Solvent Effects in Organic Chemistry*: Wiley.

Saha, B., & Abu-Omar, M. M. (2014). Advances in 5-hydroxymethylfurfural production from biomass in biphasic solvents. *Green Chemistry, 16*(1), 24-38.

Savage, P. E., Gopalan, S., Mizan, T. I., Martino, C. J., & Brock, E. E. (1995). Reactions at supercritical conditions: applications and fundamentals. *AIChE Journal, 41*(7), 1723-1778.

Seddon, K. R., Stark, A., & Torres, M.-J. (2000). Influence of chloride, water, and organic solvents on the physical properties of ionic liquids. *Pure and Applied Chemistry, 72*(12), 2275-2287.

Sener, B. (2008). *Innovations in Chemical Biology*. Netherlands: Springer.

Shi, C., Zhao, Y., Xin, J., Wang, J., Lu, X., Zhang, X., & Zhang, S. (2012). Effects of cations and anions of ionic liquids on the production of 5-hydroxymethylfurfural from fructose. *Chemical Communications, 48*(34), 4103-4105.

Shirota, H., Mandai, T., Fukazawa, H., & Kato, T. (2011). Comparison between dicationic and monocationic ionic liquids: liquid density, thermal properties, surface tension, and shear viscosity. *Journal of Chemical & Engineering Data, 56*(5), 2453-2459.

Shukla, M., Srivastava, N., & Saha, S. (2011). Interactions and transitions in imidazolium cation based ionic liquids. *Ionic Liquids-Classes and Properties*: InTech.

Ståhlberg, T., Fu, W., Woodley, J. M., & Riisager, A. (2011). Synthesis of 5-(hydroxymethyl)furfural in ionic liquids: paving the way to renewable chemicals. *ChemSusChem, 4*(4), 451-458.

Tan, S. S. Y., & MacFarlane, D. R. (2010). Ionic liquids in biomass processing. In B. Kirchner (Ed.), *Ionic Liquids* (pp. 311-339). Berlin, Heidelberg: Springer Berlin Heidelberg.

Tanaka, Ki. (1971). Toxicity of dimethylformamide (DMF) to the young female rat. *Internationales Archiv für Arbeitsmedizin, 28*(2), 95-105.

Tong, X., & Li, Y. (2010). Efficient and selective dehydration of fructose to 5-hydroxymethylfurfural catalyzed by Brønsted-acidic ionic liquids. *ChemSusChem, 3*(3), 350-355.

Tsilomelekis, G., Josephson, T. R., Nikolakis, V., & Caratzoulas, S. (2014). Origin of 5-hydroxymethylfurfural stability in water/dimethyl sulfoxide mixtures. *ChemSusChem, 7*(1), 117-126.

Tsilomelekis, G., Orella, M. J., Lin, Z., Cheng, Z., Zheng, W., Nikolakis, V., & Vlachos, D. G. (2016). Molecular structure, morphology and growth mechanisms and rates of 5-hydroxymethylfurfural (HMF) derived humins. *Green Chemistry, 18*(7), 1983-1993.

Tuteja, J., Choudhary, H., Nishimura, S., & Ebitani, K. (2014). Direct synthesis of 1, 6-hexanediol from HMF over a heterogeneous Pd/ZrP catalyst using formic acid as hydrogen source. *ChemSusChem, 7*(1), 96-100.

Van Zandvoort, I., Wang, Y., Rasrendra, C. B., van Eck, E. R. H., Bruijnincx, P. C. A., Heeres, H. J., & Weckhuysen, B. M. (2013). Formation, molecular structure, and morphology of humins in biomass conversion: influence of feedstock and processing conditions. *ChemSusChem, 6*(9), 1745-1758.

Varma, R. S., & Namboodiri, V. V. (2001). An expeditious solvent-free route to ionic liquids using microwaves. *Chemical Communications*(7), 643-644.

Vasudevan, P., Sharma, S., & Kumar, A. (2005). Liquid fuel from biomass: An overview. *Journal of Scientific & Industrial Research, 64*, 822.

Yacovitch, T. I., Wende, T., Jiang, L., Heine, N., Meijer, G., Neumark, D. M., & Asmis, K. R. (2011). Infrared spectroscopy of hydrated bisulfate anion clusters: HSO_4^- (H_2O) 1–16. *The Journal of Physical Chemistry Letters, 2*(17), 2135-2140.

Yuan, L., Feng, J., Ai, X., Cao, Y., Chen, S., & Yang, H. (2006). Improved dischargeability and reversibility of sulfur cathode in a novel ionic liquid electrolyte. *Electrochemistry Communications, 8*(4), 610-614.

Zakeeruddin, S. M., & Graetzel, M. (2009). Solvent free ionic liquid electrolytes for mesoscopic dye-sensitized solar cells. *Advanced Functional Materials, 19*(14), 2187-2202.

Zakrzewska, M. E., Bogel-Łukasik, E., & Bogel-Łukasik, R. (2011). Ionic liquid-mediated formation of 5-hydroxymethylfurfural: A Promising biomass derived building block. *Chemical Reviews, 111*(2), 397-417.

Zhang, J., & Weitz, E. (2012). An in situ NMR study of the mechanism for the catalytic conversion of fructose to 5-hydroxymethylfurfural and then to levulinic acid using ^{13}C labeled D-fructose. *ACS Catalysis, 2*(6), 1211-1218.

Zhang, Q., Ma, X., Liu, S., Yang, B., Lu, L., He, Y., & Deng, Y. (2011). Hydrophobic 1-allyl-3-alkylimidazolium dicyanamide ionic liquids with low densities. *Journal of Materials Chemistry, 21*(19), 6864-6868.

Zhang, S., Hou, Y., Huang, W., & Shan, Y. (2005). Preparation and characterization of novel ionic liquid based on benzotriazolium cation. *Electrochimica Acta, 50*(20), 4097-4103.

Zhang, X., Zhang, X., Dong, H., Zhao, Z., Zhang, S., & Huang, Y. (2012). Carbon capture with ionic liquids: overview and progress. *Energy & Environmental Science, 5*(5), 6668-6681.

Zhang, Z., &Zhao, Z. K. (2010). Microwave assisted conversion of lignocellulosic biomass into furans in ionic liquid. *Bioresource Technology, 101*(3), 1111-1114.

Zhou, Z.-B., Matsumoto, H., & Tatsumi, K. (2004). Low melting, low viscous, hydrophobic ionic liquids: 1-alkyl(alkylether)-3-methylimidazolium Perfluoroalkyltrifluoroborate. *Chemistry – A European Journal, 10*(24), 6581-6591.

LIST OF PUBLICATION AND PAPER PRESENTED

List of publication

1. Yaman, S., Mohamad, S., Manan, N.S., (2017). How do isomeric ortho, meta and para dicationic ionic liquids impact the production of 5-hydroxymethylfurfural?. *Journal of Molecular Liquids*, 238, 574-581.

List of conference

1. International Conference on Environmental and Occupational Health 2016 at Putrajaya Marriott Hotel, Malaysia on the 11-13 April 2016. (Poster presenter).